

# Journal of Visualized Experiments

## Flash Infrared Annealing for Perovskite Solar Cell Processing

--Manuscript Draft--

<b>Article Type:</b>	Invited Methods Article - JoVE Produced Video
<b>Manuscript Number:</b>	JoVE61730R2
<b>Full Title:</b>	Flash Infrared Annealing for Perovskite Solar Cell Processing
<b>Corresponding Author:</b>	Sandy Sánchez SWITZERLAND
<b>Corresponding Author's Institution:</b>	
<b>Corresponding Author E-Mail:</b>	sandy.sanchezalonso@epfl.ch
<b>Order of Authors:</b>	Sandy Sánchez Pui Sha Victoria Ling Anders Hagfeldt
<b>Additional Information:</b>	
<b>Question</b>	<b>Response</b>
Please indicate whether this article will be Standard Access or Open Access.	Open Access (US\$4,200)
Please indicate the <b>city, state/province, and country</b> where this article will be <b>filmed</b> . Please do not use abbreviations.	Lausanne/Vaud/Switzerland
Please confirm that you have read and agree to the terms and conditions of the author license agreement that applies below:	I agree to the <a href="#">UK Author License Agreement</a> (for UK authors only)
Please specify the section of the submitted manuscript.	Engineering
Please provide any comments to the journal here.	

**TITLE:**

Flash Infrared Annealing for Perovskite Solar Cell Processing

**AUTHORS AND AFFILIATIONS:**

Pui Sha Victoria Ling<sup>1,2</sup>, Anders Hagfeldt<sup>2</sup>, Sandy Sanchez<sup>2</sup>

<sup>1</sup>Department of Chemistry, Molecular Sciences Research Hub, Imperial College London, Shepherd's Bush, London, United Kingdom

<sup>2</sup>Laboratory of Photomolecular Science (LSPM), École Polytechnique Fédérale de Lausanne (EPFL), 1015 Lausanne, Switzerland

**Corresponding Authors:**

Sandy Sanchez (sandy.sanchezalonso@epfl.ch)

Anders Hagfeldt (anders.hagfeldt@epfl.ch)

**Email Address of Co-Authors:**

Pui Sha Victoria Ling ([pui.ling16@imperial.ac.uk](mailto:pui.ling16@imperial.ac.uk))

Sandy Sanchez (sandy.sanchezalonso@epfl.ch)

Anders Hagfeldt (anders.hagfeldt@epfl.ch)

**KEYWORDS:**

perovskite, solar cell, IR, rapid thermal annealing, thin film, processing, crystallization

**SUMMARY:**

We describe a flash infrared annealing method used for the synthesis of perovskite and mesoscopic-TiO<sub>2</sub> films. Annealing parameters are varied and optimized for processing on fluorine-doped tin oxide (FTO) glass and indium tin oxide-coated polyethylene terephthalate (ITO PET), subsequently giving devices power conversion efficiencies >20%.

**ABSTRACT:**

Organic-inorganic perovskites have an impressive potential for the design of next generation solar cells and are currently considered for upscaling and commercialization. Currently, perovskite solar cells rely on spin-coating which is neither practical for large areas nor environmentally friendly. Indeed, one of the conventional and most effective lab-scale methods to induce perovskite crystallization, the antisolvent method, requires an amount of toxic solvent that is difficult to apply on larger surfaces. To solve this problem, an antisolvent-free and rapid thermal annealing process called flash infrared annealing (FIRA) can be used to produce highly crystalline perovskite films. The FIRA oven is composed of an array of near-infrared halogen lamps with an illumination power of 3,000 kW/m<sup>2</sup>. A hollow aluminum body enables an effective water-cooling system. The FIRA method allows the synthesis of perovskite films in less than 2 s, achieving efficiencies >20%. FIRA has a unique potential for the industry because it can be adapted to continuous processing, is antisolvent-free, and does not require lengthy, hour-long annealing steps.

## INTRODUCTION:

Since their inception in 2009, solar cells based on lead halide perovskites have demonstrated unprecedented growth, with power conversion efficiencies (PCE) increasing from 3.8%<sup>1</sup> to 25.2%<sup>2</sup> in just over a decade of development. Recently, there has also been interest in the development of perovskite solar cells (PSCs) on flexible substrates such as polyethylene terephthalate (PET) as they are lightweight, cheap, applicable to roll-to-roll manufacturing and can be used to power flexible electronics<sup>3,4</sup>. In the past decade, the PCE of flexible PSCs has improved significantly from 2.62% to 19.1%<sup>5</sup>.

The majority of the current processing methods for PSCs involve deposition of the perovskite precursor solution, addition of an antisolvent (AS) such as chlorobenzene to induce nucleation and finally thermal annealing to evaporate the solvent and promote crystallization of the perovskite in the desired morphology<sup>6-9</sup>. This method requires moderate amounts of organic solvent (~100  $\mu$ L per 2 x 2 cm substrate) that is typically not reclaimed, is difficult to apply on large-area substrates and is not always reproducible. Additionally, the perovskite layer requires annealing at >100 °C for up to 120 min while the mesoporous-TiO<sub>2</sub> electron transporting layer requires sintering at 450 °C for at least 30 min, which not only leads to a large electronic cost and a potential bottleneck in the eventual upscaling of PSCs, but is also incompatible with flexible substrates which typically cannot sustain heating at  $\geq$ 250 °C<sup>10-12</sup>. Alternative manufacturing methods must, therefore, be found to commercialize this technology<sup>3,13,14</sup>.

Flash infrared annealing, first reported in 2015<sup>11</sup>, is a low-cost, environmentally friendly and rapid method for the synthesis of compact and defect-tolerant perovskite and metal oxide thin films that eliminates the need for an antisolvent and is compatible with flexible substrates. In this method, freshly-spin-coated perovskite films are exposed to near-IR radiation (700–2,500 nm, peaking at 1,073 nm). Both TiO<sub>2</sub> and perovskite have low absorbance in this region, whereas FTO is a strong NIR absorber and rapidly heats up, evaporating the solvent and indirectly annealing the active material<sup>11,15</sup>. A short 2 s pulse can heat the FTO substrate to 480 °C, while the perovskite remains at ~70 °C, promoting vertical evaporation of the solvent and lateral growth of crystals across the substrate. Heat is quickly dissipated via cooling from the external case, and within seconds, room temperature is reached.

The nucleation and crystallization processes, and thus the final morphology of the film, can be varied through FIRA parameters such as pulse length, frequency, and intensity, allowing for a much more reproducible and controllable crystal growth<sup>16</sup>. Assuming time-limited nucleation, the pulse length determines the nucleation density whereas the pulse intensity determines the energy provided for crystallization. Insufficient energy would result in incomplete solvent evaporation or crystallization, whereas excess energy would result in thermal degradation of the perovskite<sup>15</sup>. Optimization of these factors is, therefore, important for the formation of a homogeneous perovskite film, which can affect the optoelectronic properties of the final device.

Compared to the AS method, FIRA has a slower nucleation and faster crystal growth, leading to larger crystalline domains (~40  $\mu$ m for FIRA vs ~200 nm for AS)<sup>16</sup>. The lower nucleation rate could be due to a lower supersaturation or a limited nucleation phase as controlled by the duration of

the pulse<sup>15</sup>. However, the difference in grain size does not affect charge carrier mobility and lifetime (mobility  $\sim 15$  cm<sup>2</sup>/Vs for AS and  $\sim 19$  cm<sup>2</sup>/Vs for FIRA)<sup>17</sup> and gives films with similar structural and optical properties, as measured by X-ray diffraction (XRD) and photoluminescence (PL)<sup>12</sup>. In fact, reports suggest that larger grain sizes are favorable due to suppressed perovskite degradation at grain boundaries<sup>4</sup>. Compact, defect-tolerant, and highly crystalline perovskite films can be formed with both methods, giving devices with >20% PCE<sup>18</sup>.

Additionally, the elimination of the antisolvent and the reduction in annealing time from hours to seconds make it much more cost-effective and environmentally friendly. With this method, a crystalline mesoscopic-TiO<sub>2</sub> layer can also be manufactured, reducing the energy-intensive sintering step (at 450 °C for 30 min, 1–3 h in total) to just 10 min<sup>16,18</sup>. TiO<sub>2</sub> annealing times as short as seconds have also been previously reported using variations of this method<sup>19–22</sup>. As a result, a whole PSC can be fabricated in less than an hour<sup>18</sup>. This method is also compatible with industrial upscaling and commercialization as it can be adapted to large-area deposition and roll-to-roll processing for fast and synchronized throughput production<sup>15</sup>. Furthermore, the water-cooling system allows rapid heat dissipation, making it suitable for the fabrication of devices on flexible substrates such as PET.

FIRA can be used for any wet, thin film that can be deposited via a simple solution process and crystallized at different temperatures up to 1,000 °C. The parameters can be optimized such that crystals in the desired morphology are formed. For example, it has been used for the synthesis of various perovskite compositions on glass and PET<sup>12,15,18</sup>, as well as the mesoscopic-TiO<sub>2</sub> layer on glass, giving devices of >20% PCE<sup>18</sup>. It also allows for the study of phase evolution against temperature, as the oven and substrate surface temperatures are measured to give a temperature profile of the crystallization process<sup>16,17</sup>.

This paper firstly discusses the protocol used for the optimization of annealing parameters to synthesize a compact, defect-tolerant, and homogeneous perovskite (MAPbI<sub>3</sub>) film, which simultaneously offers insight into perovskite morphology evolution against temperature/pulse time. Secondly, a protocol for the processing of perovskite solar cells with FIRA-annealed mesoscopic-TiO<sub>2</sub> and perovskite layers is discussed. For this study, a perovskite composition based on formamidinium (80%), caesium (15%), and guanidinium (5%) cations was used (herein denoted FCG), and a tetrabutyl ammonium iodide (TBAI) post-treatment was carried out. Therefore, this paper aims to demonstrate the versatility of the FIRA method, its advantages over the conventional antisolvent method, and its potential to be applied in the eventual commercialization of perovskite solar cells<sup>20–22</sup>.

This protocol is divided into 4 sections: 1) A general description of the operation of the FIRA oven 2) Process for the optimization and synthesis of a MAPbI<sub>3</sub> perovskite film on FTO glass 3) Processing of FCG perovskite solar cells and 4) Synthesis of MAPbI<sub>3</sub> films on ITO-PET.

## **PROTOCOL:**

### **1. Operation of the FIRA Oven**

NOTE: A schematic of the FIRA oven, developed in-house, is shown in **Figure 1A**. The FIRA oven is composed of an array of six near-infrared halogen lamps (peak emission at wavelength of 1,073 nm) with an illumination power of 3,000 kW/m<sup>2</sup> and a total output power of 9,600 kW. A hollow aluminum body provides an effective water-cooling system and it in turn allows rapid thermal energy dissipation (within seconds). It is kept in a nitrogen glovebox, and N<sub>2</sub> is continuously flowed through the chamber via a gas inlet to keep it under an inert atmosphere, except during annealing. O<sub>2</sub> can also be introduced when annealing metal oxide films to promote oxidation.

[Insert **Figures 1 and 2** here]

## 1.1 Programming of annealing cycles

1.1.1 Connect the FIRA oven to a computer, from which it can be controlled via a guide user interface (**Figure 2**) on an in-house software. Based on the experiment, select full-power mode or PID (proportional-integral-derivative) mode. In full-power mode, the IR lamps are either completely on or off, whereas in PID mode, the oven is held at a specific temperature for a certain amount of time by intensity modulation.

1.1.2 Ensure **Table** is selected on the **Table/Manual** toggle and input a timebase that is longer than the total duration of the annealing and cooling processes.

1.1.3 **Full-power mode:** Input the times at which the lamps should be on or off in the table on the right of the interface. In this way, single pulses as well as annealing cycles can be programed, allowing control of the pulse length and frequency. This is suitable for films that can be rapidly annealed, or for substrates that cannot tolerate sustained heating (e.g ,~1.5–2 s for perovskite films).

1.1.4 **PID mode:** Input the time and temperature at which the oven should be irradiated in the table. Similar to the working principle of a traditional hotplate, the intensity of the heating source can be modulated. This is suitable for films that typically require longer annealing times (e.g., 15 min at 100 °C for TBAI).

1.1.5 **Data acquisition:** Download the temperature profile displayed on the left of the interface as a .txt or spreadsheet file by right-clicking on the profile and then click on **Export File**.

NOTE: The software is used for both data acquisition and system control, where the main raw data acquired is the temperature profile. On the temperature profile (**Figure 2**), the input program is represented by the “set point”. The oven temperature (measured by a K-type thermocouple) and substrate temperature (estimated by a pyrometer) are displayed in real time, giving insight into the thin film crystallization conditions. Please note that the oven temperature does not scale directly with traditional hot plate temperatures as the thermocouple is also directly exposed to IR radiation. Rather, it serves as a reference point for comparison between different FIRA annealing parameters.

## 1.2 General annealing process

1.2.1 Deposit the precursor via a suitable solution process: spin-coating<sup>26</sup>, dip-coating<sup>27</sup>, or doctor-blading<sup>28</sup>.

1.2.2 Transfer the substrates into the FIRA oven chamber and close the oven lid. Ensure that nitrogen flow into the chamber is turned off by closing the gas inlet valve.

1.2.3 Start and stop the annealing by clicking on **START table** and **STOP table** on the computer. Alternatively, connect the FIRA oven to a foot pedal, which can also be used to start and stop the program. As a result, annealing can be carried out without removing one's hands from the glovebox, allowing for a much smoother and synchronized process.

1.2.4 When the oven temperature reaches the room temperature, remove the substrates from the oven chamber.

## 2. MAPbI<sub>3</sub> Perovskite Film Synthesis and Optimization on FTO Glass

### 2.1 Perovskite Solution Preparation

2.1.1 Dissolve methylammonium iodide in anhydrous DMF:DMSO 2:1 v/v to obtain a 1.9 M solution.

2.1.2 Add an equimolar amount of PbI<sub>2</sub> to the solution and dilute with anhydrous DMF:DMSO 2:1 v/v to give a 1.4 M methylammonium lead iodide precursor solution. Heat at 80 °C until complete dissolution and cool to room temperature.

NOTE: The solution is prepared and stored in an argon glovebox. The protocol can be paused here.

### 2.2 Perovskite film synthesis

2.2.1 Use FTO coated glass substrates of 1.7 cm x 2.5 cm.

2.2.2 Clean the substrates via successive sonication in cleaning soap (2 vol % in deionized H<sub>2</sub>O), acetone and ethanol for 15 min each, then dry them with compressed air.

2.2.3 Treat the substrates under UV/ozone in a plasma cleaner for 15 min.

2.2.4 Input the desired annealing program as per section 1.1.

2.2.5 Blow the substrate surface with a nitrogen gun to remove dust and other impurities.

2.2.6 Spin-coat 50  $\mu\text{L}$  of the perovskite precursor at 4,000 rpm for 10 s, with an acceleration of 2000  $\text{rpm}\cdot\text{s}^{-1}$ .

2.2.7 Immediately after deposition, transfer the substrate to the FIRA oven for annealing at a range of pulse times as desired (0–7 s used herein, optimized pulse is 2 s). Start the inputted annealing program by pressing **START** on the software or stepping on the foot pedal. A color change from yellow to black should be observed, indicating the formation of a 3D perovskite structure.

2.2.8 Remove the substrate when the oven temperature reaches 25  $^{\circ}\text{C}$ .

2.2.9 Store the annealed films in a dry air box.

NOTE: The FIRA oven and the spin-coater are placed in the same nitrogen glovebox such that solution deposition and annealing can be carried out smoothly and under an inert atmosphere.

## 2.3 Material characterization

2.3.1 Capture optical images on a polarizing microscope equipped with a xenon light source and infinitely corrected objectives of 10x and 50x.

2.3.2 Record absorbance spectra simultaneously with an optical fiber integrated into the microscope set-up and connected to a spectrometer (spectral range 300–1,100 nm).

NOTE: The above characterization can be done immediately after annealing, allowing for rapid screening of film quality. The measurements are taken in ambient air and temperature. More in-depth characterization such as scanning electron microscopy (SEM) and X-ray diffraction can be subsequently carried out (see section 3.7).

## 3. FCG perovskite solar cell processing

### 3.1 Substrate preparation and cleaning

3.1.1 Etch one side of the FTO glass substrates with Zn powder and 4 M HCl.

3.1.2 Clean substrates via successive sonication in cleaning soap (2 vol % in deionized  $\text{H}_2\text{O}$ ) for 30 min and isopropanol for 15 min, and dry with compressed air.

3.1.3 Treat under UV/ozone in a plasma cleaner for 5 min.

### 3.2 Compact $\text{TiO}_2$ layer

3.2.1 Heat FTO glass substrates to 450  $^{\circ}\text{C}$  on a sintering hot plate and keep them at this temperature for 15 min before solution deposition.

3.2.2 Dilute 0.6 mL of titanium diisopropoxide bis(acetylacetonate) and 0.4 mL of acetylacetone in 9 mL of EtOH to give the precursor solution.

3.2.3 Deposit the solution via spray pyrolysis with oxygen as the carrier gas (0.5 bar) at 45° and a distance of ~20 cm. Leave an interval of 20 s between each spraying cycle.

3.2.4 Leave the substrates at 450 °C for 5 min more, then cool to room temperature. This gives a compact TiO<sub>2</sub> layer of ~30 nm.

NOTE: The protocol can be paused here. If the next step is not carried out immediately, re-sinter the substrate at 450 °C for 30 min before deposition of the mesoporous-TiO<sub>2</sub> layer.

### 3.3 Mesoporous-TiO<sub>2</sub> layer

3.3.1 Make a precursor solution by diluting TiO<sub>2</sub> paste (particle size 30 nm) in EtOH at a concentration of 75 mg/mL. Stir the solution with a magnetic stirrer bar until complete dissolution.

3.3.2 Spin-coat 50 µL of the solution at 4,000 rpm for 10 s, with a ramp of 2,000 rpm·s<sup>-1</sup>.

3.3.3 Program an annealing cycle of 10 pulses, 15 s on and 45 s off in the table on the software.

3.3.4 Place the substrates in the FIRA oven, and anneal under full power mode with the above annealing cycle by pressing **Start Table** or stepping on the foot pedal. This yields a 150–200 nm layer.

3.3.5 Remove the samples when the oven temperature reaches 25 °C.

NOTE: Ensure that the oven is at room temperature or below before starting annealing. With the above cycle, the oven temperature reaches ~600 °C during annealing.

### 3.4 Perovskite layer

3.4.1 Make a solution of formamidinium iodide (1.12 M), PbI<sub>2</sub> (1.4 M), CsI (0.21 M) and GAI (0.07 M) in anhydrous DMF:DMSO 2:1 v/v.

3.4.2 Spin-coat 40 µL of the solution at 4,000 rpm for 10 s.

3.4.3 Program an annealing step of 1.6 s on full power mode on the software (until it reaches 90 °C).

3.4.4 Transfer the substrate to the FIRA oven and start annealing by pressing **Start Table** or stepping on the foot pedal. The surface should turn from yellow to black.



3.4.5 Leave the samples in the oven for an additional 10 s for cooling before removal.

3.5 Tetrabutyl ammonium iodide (TBAI) post-treatment (optional)

3.5.1 Dissolve 3 mg of tetrabutyl ammonium iodide in 1 mL of isopropanol.

3.5.2 Spin-coat the solution at 4,000 rpm for 20 s.

3.5.3 Program an annealing step at 100 °C for 15 min using PID mode.

3.5.4 Transfer the substrate to the FIRA oven and anneal with the above program. Cool to 25 °C before the next step.

3.6 Hole transporting material and top electrode

3.6.1 Dissolve spiro-OMeTAD in chlorobenzene (70 mM) and add 4-tert-butylpyridine (TBP), Lithium bis(trifluoromethylsulfonyl)imide) (Li-TFSI, 1.8 M in acetonitrile) and Tris(2-(1H-pyrazol-1-yl)-4-tert-butylpyridine)-cobalt(III) Tris(bis(trifluoromethylsulfonyl) imide) (FK209, 0.25 M in acetonitrile) such that the molar ratio of the additives with respect to spiro-OMeTAD are 3.3, 0.5, and 0.03 for TBP, Li-TFSI, and FK209 respectively.

3.6.2 Deposit 50 µL of the solution at 4,000 rpm for 20 s under dynamic spin-coating, adding the solution 3 s after the start of the program.

3.6.3 Leave it to oxidize overnight in a dry air box.

3.6.4 Deposit 80 nm of gold via thermal evaporation under vacuum. Use a shadow mask to pattern the electrodes.

3.7 Photovoltaic device testing and material characterization

3.7.1 Take photovoltaic measurements using a solar simulator equipped with a xenon arc lamp and a digital source meter. Specify the active area of the device with a black, non-reflective metal mask (0.1024 cm<sup>2</sup> used herein). Measure the current-voltage curves under reverse and forward bias at a 10 mV/s scan rate under AM 1.5 G irradiation.

3.7.2 Take X-ray diffraction patterns with a diffractometer in reflection-spin mode, using Cu K $\alpha$  radiation and a Ni  $\beta$  filter.

3.7.3 Take scanning electron microscope images at an acceleration voltage of 3 kV.

#### 4. MAPbI<sub>3</sub> films on ITO-PET substrate

- 4.1 Cut ITO-PET and microscope glass slides into pieces of 1.7 cm x 2.5 cm.
- 4.2 Clean the glass slides and ITO-PET as per steps 2.2.2–2.2.3.
- 4.3 Attach the ITO substrates onto the glass slides with double-sided tape, ensuring they are as flat as possible.
- 4.4 Prepare the MAPbI<sub>3</sub> precursor as described in section 2.1. Blow the substrate surface with an N<sub>2</sub> gun before spin-coating the solution and annealing the film with FIRA, as per steps 2.2.5–2.2.8, with a pulse time of 1.7 s.
- 4.5 Carry out material characterization as described in sections 2.3 and 3.7.

## REPRESENTATIVE RESULTS:

### Optimization and synthesis of MAPbI<sub>3</sub> films on FTO glass

To assess perovskite film quality, microscope images, X-ray diffraction, and absorbance spectra were taken. The optimum pulse time should yield a compact, uniform, and pinhole-free film with large crystal grains. **Figure 3** shows optical images of MAPbI<sub>3</sub> films at pulse times ranging from 0 s to 7 s, while **Figure 4** shows the XRD spectra of films annealed at selective pulse times. These pulse times represent the boundaries of the four distinct perovskite phases observed based on the various characterizations carried out. The phase evolution as a function of pulse time and temperature is shown in **Figure 5**, and a comparison of the top-view SEM images of films formed by both FIRA and antisolvent methods are found in supplementary information S1. XRD patterns for all pulses and corresponding absorbance spectra are found in supplementary information S2 and S3. Pulses from 0 to 1.6 s gave needle-like crystals or small crystalline domains separated by non-crystalline phases, as evidenced by the precursor peaks at  $2\theta = 6.59, 7.22, \text{ and } 9.22^\circ$ <sup>29</sup>. For 1.8 to 3.8 s pulses, well-defined crystal grains were formed, and XRD patterns showed the formation of the MAPbI<sub>3</sub> tetragonal I4/mcm phase. This is also confirmed by the absorption onset of 780 nm. However, longer pulse times led to thermal degradation of the perovskite, with complete degradation for pulses >5 s, as shown by the evolution of the PbI<sub>2</sub> peak at  $2\theta = 12.7^\circ$ . The optimized pulse was determined to be 2 s, giving crystal grains of ~30  $\mu\text{m}$ . Therefore, FIRA allows for a comprehensive study of the nucleation and crystallization processes based on temperature, as controlled by the pulse time. The parameters can also be varied and optimized for different thin films, showing the versatility of this method.

[Insert Figures 3–5 here]

### FCG perovskite devices

**Figures 6A,B** show the temperature profile and XRD pattern of the mesoscopic-TiO<sub>2</sub> layer annealed with a FIRA cycle of 10 pulses, 15 s on and 45 s off. With FIRA, temperatures of ~600 °C could be reached and the TiO<sub>2</sub> layer can be synthesized in just 10 min, much shorter than the conventional method which requires sintering for 1 h to 3 h, peaking at 450 °C. The resulting film shows no discernible difference to that sintered on a hot plate. As a result, the whole perovskite

solar cell could be processed in less than an hour. The cross-sectional SEM image (**Figure 6C**) shows that the subsequent devices fabricated are very similar to those made via traditional methods, with layers of similar thickness and morphology. Additionally, FIRA-processed devices showed excellent performance (**Figure 7**), with the champion device showing PCE = 20.1%, FF = 75%,  $V_{oc}$  = 1.1 V, and  $J_{sc}$  = 24.4 mA/cm<sup>2</sup>, comparable to devices fabricated with the antisolvent method. A large-area device with a 1.4 cm<sup>2</sup> active area also gave PCE of 17%, showing FIRA is a promising alternative processing method for the manufacture of PSCs.

[Insert Figure 6-7 here]

#### MAPbI<sub>3</sub> films on ITO-PET

**Figure 8** shows optical images of MAPbI<sub>3</sub> films annealed at pulses ranging from 1 s to 2 s. At shorter pulse times, there is incomplete crystallization, whereas at pulse times >1.7 s, the PET substrate begins to melt (see **Supplemental Figure 4**). Thermal degradation of the perovskite is also observed for the 2 s pulse. At the optimized pulse time of 1.7 s, densely packed crystal domains of ~15 μm were observed. Although there are small pinholes of 1–2 μm, it is clear that FIRA can be used to form compact and uniform perovskite films on flexible polymers without melting the substrate, due to rapid cooling from the case, which is a significant advantage compared to hotplate annealing.

[Insert Figure 7–8 here]

#### FIGURE AND TABLE LEGENDS:

**Figure 1: (A) Schematic showing cross-section of the FIRA oven.** The oven chamber is continuously cooled by water flowing through the case and kept under an N<sub>2</sub> atmosphere. **(B) Picture of the FIRA oven.**

**Figure 2: Interface of the FIRA software.** The panel on the left shows the temperature profile, which displays the set point (input program), oven temperature, and pyrometer (substrate surface) temperature. The desired annealing program is inputted on the table on the right.

**Figure 3: Optical images of MAPbI<sub>3</sub> perovskite films on FTO glass,** annealed with pulses ranging from 0 s to 7 s. All images were taken at 10x magnification in transmission mode.

**Figure 4: XRD spectra of MAPbI<sub>3</sub> films annealed at selective pulse times.** Labeled planes are representative of the tetragonal I4/mcm phase. Asterisked peaks represent diffractions from PbI<sub>2</sub>, while the blue rectangle represents those from the precursor solution.

**Figure 5: Temperature profile showing perovskite phase evolution as a function of pulse length.** The boundary of the different phases has been determined from the corresponding XRD analysis, shown in **Figure 4**. Adapted from<sup>15</sup>.

**Figure 6: (A)** Temperature profile of mesoporous TiO<sub>2</sub> annealing in FIRA, with a cycle of 10 pulses of 15 s on and 45 s off. **(B)** X-ray patterns for TiO<sub>2</sub> films annealed with a hotplate and FIRA, and a blank FTO substrate as reference. **(C)** Cross-sectional SEM images of perovskite solar cell architectures, processed by FIRA and antisolvent. Reproduced with permission from<sup>18</sup>.

**Figure 7: Current-voltage curve for champion FCG perovskite devices. (A)** FIRA-annealed mesoporous-TiO<sub>2</sub> and perovskite layers. **(B)** Large area (1.4 cm<sup>2</sup>) device with FIRA-annealed mesoporous-TiO<sub>2</sub> and perovskite layers. Reproduced with permission from<sup>18</sup>.

**Figure 8: Optical images of MAPbI<sub>3</sub> films annealed at various pulse times on ITO-PET.** All images are taken in transmission mode and 10x magnification unless otherwise specified.

**Figure 9: Schematic representation of perovskite film processing with FIRA.** The wet film is deposited from the solution by spin-coating and subsequently transferred to the FIRA oven for annealing in ~2 s, giving the black perovskite stable phase.

**Figure 10: A comparison of the relative cost and environmental impact of FIRA and anti-solvent methods determined by life cycle assessment.** GWP = Climate change [kg CO<sub>2</sub> eq], POP = Photochemical oxidation [kg C<sub>2</sub>H<sub>4</sub> eq], AP = Acidification [kg SO<sub>2</sub> eq], CED = Cumulative energy demand [MJ], HTC = Human Toxicity, cancer effects [CTUh], HTNC = Human Toxicity, non-cancer effects [CTUh], ET = Freshwater ecotoxicity [CTUe]. Reproduced with permission from<sup>12</sup>.

**Supplemental Figure 1: Top-view SEM comparison of FIRA and hotplate annealed perovskite films. (A)** Top view of FIRA-annealed perovskite films for four annealing times, scale bar: 25 μm. **(B)** Top view of a reference film made by the antisolvent method followed by annealing at 100 °C for 1 h on a standard hotplate, scale bar: 1 μm. Adapted from<sup>1</sup>.

**Supplemental Figure 2: XRD spectra of MAPbI<sub>3</sub> films on FTO glass, annealed with pulses of (A)** 0–1.4 s **(B)** 1.6–3 s **(C)** 3.2–4.6 s **(D)** 4.8–7 s.

**Supplemental Figure 3: Absorbance spectra of MAPbI<sub>3</sub> films on FTO glass, annealed with pulses of (A)** 0.2–1.8 s **(B)** 2–3.6 s **(C)** 3.8–7 s.

**Supplemental Figure 4: Physical appearance of MAPbI<sub>3</sub> films annealed on PET at various pulse lengths.**

**Supplemental Figure 5: Temperature profile and top-view SEM images of the pristine paper substrate, ITO electrode, and mesoporous-TiO<sub>2</sub> layer processed with FIRA.**

**Supplemental Figure 6: Cross-sectional SEM image of perovskite deposited (via antisolvent method) on a FIRA-annealed ITO/TiO<sub>2</sub> stack.** ITO np = ITO nanoparticles, pvk = perovskite.

## DISCUSSION:

**Figure 9** shows the general process of perovskite film annealing with FIRA.

[Insert Figure 9 here]

In the solidification process of a thin film from the solution, the desired final shape will depend on the application: films in energy devices for photocatalysis, battery electrodes, and solar cells can have different morphologies<sup>30–33</sup>. Therefore, identifying the optimal parameters for each substrate and wet film interface is a critical step in the protocol to follow. Typically, for PSCs we expect to have shiny and smooth films in order to minimize defects and to enhance the photophysical properties such as charge transport of carriers to give null non-radiative recombination<sup>34,35,36</sup>. For thin film processing, the main parameters are pulse time, the number of pulses, and the irradiation temperature, which are a balance between forming the desired morphology while being as rapid and energy efficient as possible. Insufficient energy would lead to incomplete solvent evaporation or crystallization, while excess energy would lead to degradation of the material. Therefore, it is crucial to systematically vary the annealing parameters and analyze the resulting film quality (as detailed in sections 2.2, 2.3, and 3.7) to find the optimal parameters for each thin film/substrate combination. Once this is completed, thin films can be synthesized rapidly and reliably. The method relies on its accuracy, for example, the minimum pulse time is 20 ms, allowing one to finely control the temperature ratio for crystal growth. Besides, one can have a wide window for optimization, aided by the data collection of images and absorption spectra for optical and morphological screening.

The FIRA method is still in development, and, as its name implies, it is currently based on IR irradiation. However, the latest version of FIRA includes UV-A radiation generated from a separate metal-halide lamp source. UV and IR can be used for combined wavelength photonic annealing and curing, providing additional functionality. For example, semiconductor curing with FIRA is a straightforward way to improve the wettability of substrates. Additionally, for a multi-layered approach in crystal growth, this selective wavelength annealing can be adapted depending on the material, and the pulse can be modulated depending on the desired shape<sup>16,32,37</sup>. Current investigations include annealing of an ITO electrode and a mesoscopic-TiO<sub>2</sub> layer on paper (the latter using mixed IR/UV annealing, see **Supplemental Figure 5** in the supplementary information). As shown in **Supplemental Figure 6**, a perovskite film can be successfully deposited on the FIRA-annealed ITO/TiO<sub>2</sub> stack. This can be applied to a wide range of substrates and thin films in the future.

So far, the FIRA method is limited to the annealing of wet films that can be deposited via solution processes. It depends on the capability of the deposition method, and this is governed by solvent engineering and multi-layered growth based on solutions with approaching solvent polarities. Optimization is also required for each thin film as this is a novel method without a lot of previously reported protocols in literature, which may be time-consuming. Additionally, although FIRA can be used for flexible substrates such as PET and paper as there is rapid cooling from the case, a good contact between the substrate and the oven chamber must be ensured to avoid substrate melting. This may be difficult since flexible substrates are easily bent during processing, but this may be improved by attaching the substrates on a thin glass slide to ensure that they are completely flat and to allow ease of manipulation. However, it is important to note that the

absorption of the film will change as the material transitions from non-absorbing (wet NIR-transparent perovskite precursor material) to dry (NIR-absorbing black perovskite) and this additional absorption can contribute to the damage of the substrate<sup>38</sup>.

Despite these limitations, FIRA still presents many advantages in comparison to the antisolvent method. Firstly, thin films can be synthesized much quicker. For example, the perovskite is formed in <2 s while the mesoporous-TiO<sub>2</sub> layer is formed in only 10 min, much shorter than the hours required in the conventional method. The elimination of the antisolvent and the shorter annealing times also mean that there is a much lower energetic and financial cost. Life cycle assessment (**Figure 10**) of the perovskite synthesis process shows that FIRA presents only 8% of the environmental impact and 2% of the fabrication cost of the antisolvent method. Additionally, it is compatible with flexible and large-area substrates. A total area of 10 x 10 cm<sup>2</sup> can be irradiated at one time, and it has already been shown that devices of 1.4 cm<sup>2</sup> active area as well as films of 100 cm<sup>2</sup> can be synthesized this way. Finally, it is highly reproducible, versatile, and adaptable to fast throughput roll-to-roll manufacturing, as the deposition and annealing steps are carried out continuously in one place in a synchronized and smooth process.

**[Insert Figure 10 here]**

Current investigations on FIRA are focused on optimization for thin film synthesis on flexible substrates such as paper and PET, as well as for the synthesis of other key component layers of PSCs such as the SnO<sub>2</sub> compact layer, or carbon and ITO electrodes. Furthermore, the next step is to fabricate high-performing devices of >5 cm<sup>2</sup>. Therefore, it can be said that FIRA represents a step toward an environmentally friendly and cost-efficient way to manufacture large-area, commercial PSCs.

#### **ACKNOWLEDGMENTS:**

The project (WASP) leading to this publication, has received funding from the European Union's Horizon 2020 Research and Innovation Program under grant agreement No. 825213.

#### **DISCLOSURES:**

The authors have nothing to disclose.

#### **REFERENCES:**

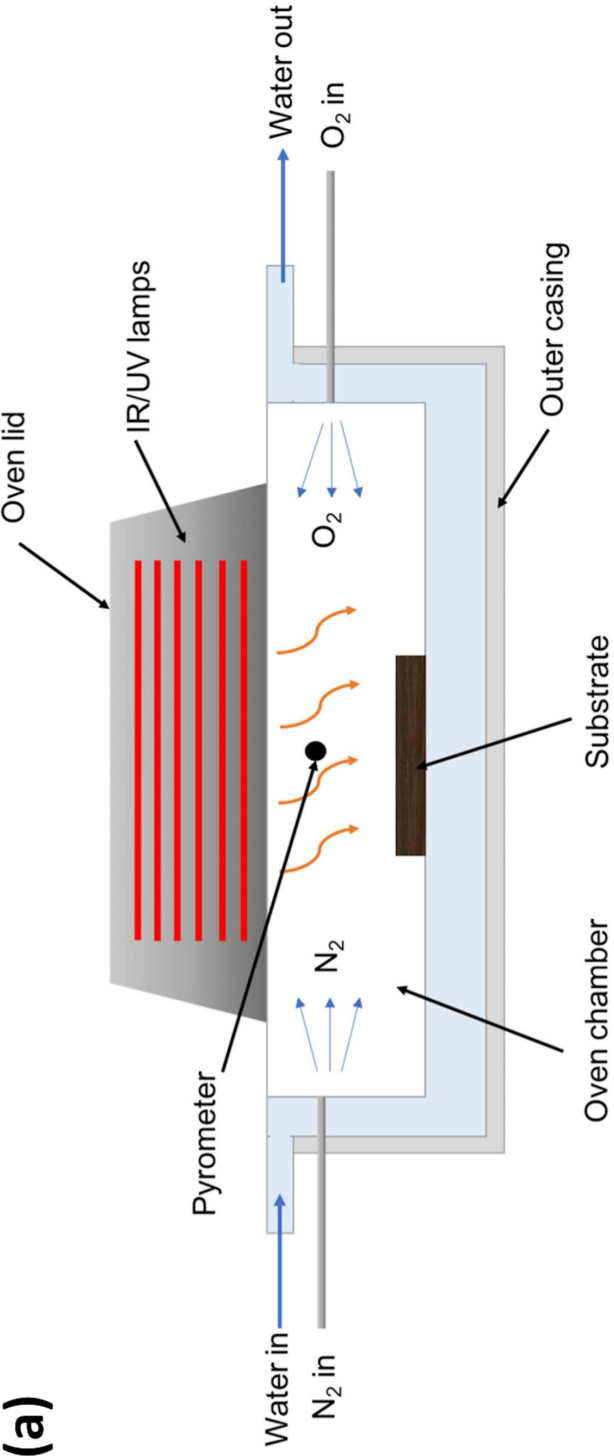
1. Kojima, A., Teshima, K., Shirai, Y., Miyasaka, T. Organometal halide perovskites as visible-light sensitizers for photovoltaic cells. *Journal of the American Chemical Society*. **131** (17), 6050–6051 (2009).
2. National Renewable Energy Laboratory. Best Research-Cell Efficiency Chart <https://www.nrel.gov/pv/assets/pdfs/best-research-cell-efficiencies.20200406.pdf> (accessed Apr 12, 2020).
3. Mujahid, M., Chen, C., Hu, W., Wang, Z.-K., Duan, Y. Progress of high-throughput and low-cost flexible perovskite solar cells. *Solar RRL*. **4**, 1900556 (2020).
4. Feng, J. et al. Record efficiency stable flexible perovskite solar cell using effective additive assistant strategy. *Advanced Materials*. **30** (35), 1–9 (2018).

- 572 5. Cao, B. et al. Flexible quintuple cation perovskite solar cells with high efficiency. *Journal*  
573 *of Materials Chemistry A*. **7** (9), 4960–4970 (2019).
- 574 6. Green, M. A., Ho-Baillie, A., Snaith, H. J. The emergence of perovskite solar cells. *Nature*  
575 *Photonics*. **8** (7), 506–514 (2014).
- 576 7. Park, N.-G. Perovskite solar cells: an emerging photovoltaic technology. *Materials Today*.  
577 **18** (2), 65–72 (2015).
- 578 8. Zhou, H. et al. Interface engineering of highly efficient perovskite solar cells. *Science*. **345**  
579 (6196), 542–546 (2014).
- 580 9. Jeon, N. J. et al. Compositional engineering of perovskite materials for high-performance  
581 solar cells. *Nature*. **517** (7535), 476–480 (2015).
- 582 10. Troughton, J. et al. Photonic flash-annealing of lead halide perovskite solar cells in 1 Ms.  
583 *Journal of Materials Chemistry A*. **4** (9), 3471–3476 (2016).
- 584 11. Troughton, J. et al. Rapid processing of perovskite solar cells in under 2.5 seconds. *Journal*  
585 *of Materials Chemistry A*. **3** (17), 9123–9127 (2015).
- 586 12. Sánchez, S. et al. Flash infrared annealing as a cost-effective and low environmental  
587 impact processing method for planar perovskite solar cells. *Materials Today*. **31**, 39–46 (2019).
- 588 13. Park, N.-G., Grätzel, M., Miyasaka, T., Zhu, K., Emery, K. Towards stable and commercially  
589 available perovskite solar cells. *Nature Energy*. **1** (11), 16152 (2016).
- 590 14. Song, Z. et al. A technoeconomic analysis of perovskite solar module manufacturing with  
591 low-cost materials and techniques. *Energy & Environmental Science*. **10** (6), 1297–1305 (2017).
- 592 15. Sanchez, S., Hua, X., Phung, N., Steiner, U., Abate, A. Flash infrared annealing for  
593 antisolvent-free highly efficient perovskite solar cells. *Advanced Energy Materials*. **8**, 1702915  
594 (2018).
- 595 16. Sánchez, S. et al. Flash infrared pulse time control of perovskite crystal nucleation and  
596 growth from solution. *Crystal Growth & Design*. **20** (2), 670–679 (2020).
- 597 17. Muscarella, L. A. et al. Crystal orientation and grain size: do they determine optoelectronic  
598 properties of MAPbI<sub>3</sub> perovskite? *The Journal of Physical Chemistry Letters*. **10** (20), 6010–6018  
599 (2019).
- 600 18. Sánchez, S., Jerónimo-Rendon, J., Saliba, M., Hagfeldt, A. Highly efficient and rapid  
601 manufactured perovskite solar cells via flash infraRed annealing. *Materials Today*. In Press (2020).
- 602 19. Watson, T., Mabbett, I., Wang, H., Peter, L., Worsley, D. Ultrafast near infrared sintering  
603 of TiO<sub>2</sub> layers on metal substrates for dye-sensitized solar cells. *Progress in Photovoltaics:*  
604 *Research and Applications*. **19** (4), 482–486 (2011).
- 605 20. Hooper, K., Carnie, M. J., Charbonneau, C., Watson, T. Near infrared radiation as a rapid  
606 heating technique for TiO<sub>2</sub> films on glass mounted dye-sensitized solar cells. *International Journal*  
607 *of Photoenergy*. 953623 (2014).
- 608 21. Carnie, M. J. et al. Ultra-fast sintered TiO<sub>2</sub> films in dye-sensitized solar cells: phase  
609 variation, electron transport and recombination. *Journal of Materials Chemistry A*. **1** (6), 2225–  
610 2230 (2013).
- 611 22. Baker, J. et al. High throughput fabrication of mesoporous carbon perovskite solar cells.  
612 *Journal of Materials Chemistry A*. **5** (35), 18643–18650 (2017).
- 613 23. Berhe, T. A. et al. Organometal halide perovskite solar cells: degradation and stability.  
614 *Energy & Environmental Sciences*. **9** (2), 323–356 (2016).
- 615 24. Jung, H. S., Park, N.G. Perovskite solar cells: from materials to devices. *Small*. **11** (1), 10–

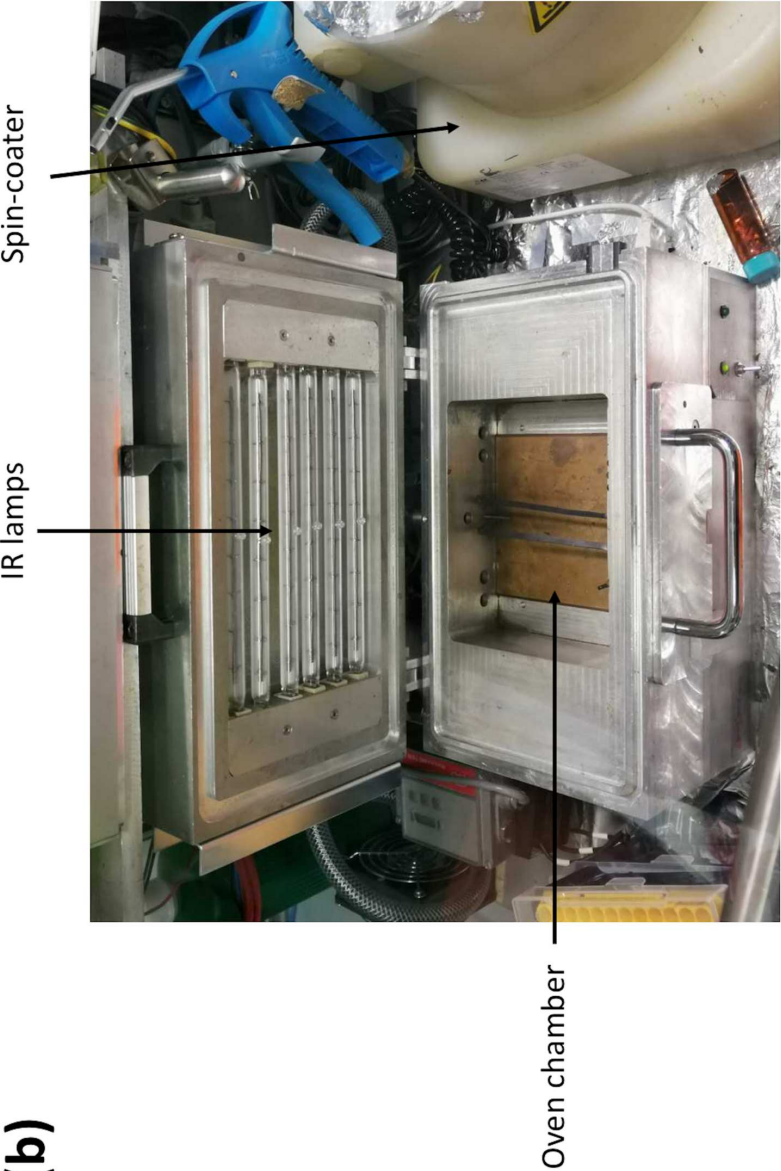
- 25 (2015).
25. Burschka, J. et al. Sequential Deposition as a route to high-performance perovskite-sensitized solar cells. *Nature*. **499** (7458), 316–319 (2013).
26. Xiao, M. et al. A fast deposition-crystallization procedure for highly efficient lead iodide perovskite thin-film solar cells. *Angewandte Chemie International Edition*. **53** (37), 9898–9903 (2014).
27. Adnan, M., Lee, J. K. All sequential dip-coating processed perovskite layers from an aqueous lead precursor for high efficiency perovskite solar cells. *Scientific Reports*. **8** (1), 2168 (2018).
28. Santa-Nokki, H., Kallioinen, J., Kololuoma, T., Tuboltsev, V., Korppi-Tommola, J. Dynamic preparation of TiO<sub>2</sub> films for fabrication of dye-sensitized solar cells. *Journal of Photochemistry and Photobiology A: Chemistry*. **182** (2), 187–191 (2006).
29. Sanchez, S., Steiner, U., Hua, X. Phase evolution during perovskite formation—insight from pair distribution function analysis. *Chemistry of Materials*. **31** (9), 3498–3506 (2019).
30. Virkar, A. A., Mannsfeld, S., Bao, Z., Stingelin, N. Organic semiconductor growth and morphology considerations for organic thin-film transistors. *Advanced Materials*. **22** (34), 3857–3875 (2010).
31. Hoppe, H., Sariciftci, N. S. Morphology of polymer/fullerene bulk heterojunction solar cells. *Journal of Materials Chemistry*. **16** (1), 45–61 (2006).
32. Paquin, F., Rivnay, J., Salleo, A., Stingelin, N., Silva, C. Multi-phase semicrystalline microstructures drive exciton dissociation in neat plastic semiconductors. *Journal of Materials Chemistry C*. **3** (41), 10715–10722 (2015).
33. Diao, Y., Shaw, L., Bao, Z., Mannsfeld, S. C. B. Morphology control strategies for solution-processed organic semiconductor thin films. *Energy & Environmental Sciences*. **7** (7), 2145–2159 (2014).
34. Slotcavage, D. J., Karunadasa, H. I., McGehee, M. D. Light-induced phase segregation in halide-perovskite absorbers. *ACS Energy Letters*. **1** (6), 1199–1205 (2016).
35. Jiang, Q. et al. Surface passivation of perovskite film for efficient solar cells. *Nature Photonics*. **13** (7), 460–466 (2019).
36. Yang, W. S. et al. Iodide Management in formamidinium-lead-halide-based perovskite layers for efficient solar cells. *Science*. **356** (6345), 1376–1379 (2017).
37. Almadhoun, M. N., Khan, M. A., Rajab, K., Park, J. H., Buriak, J. M., Alshareef, H. N. UV-Induced ferroelectric phase transformation in PVDF thin films. *Advanced Electronic Materials*. **5** (1), 1800363 (2019).
38. Hooper, K., Smith, B., Baker, J., Greenwood, P., Watson, T. Spray PEDOT:PSS coated perovskite with a transparent conducting electrode for low cost scalable photovoltaic devices. *Materials Research Innovations*. **19** (7), 482–487 (2015).

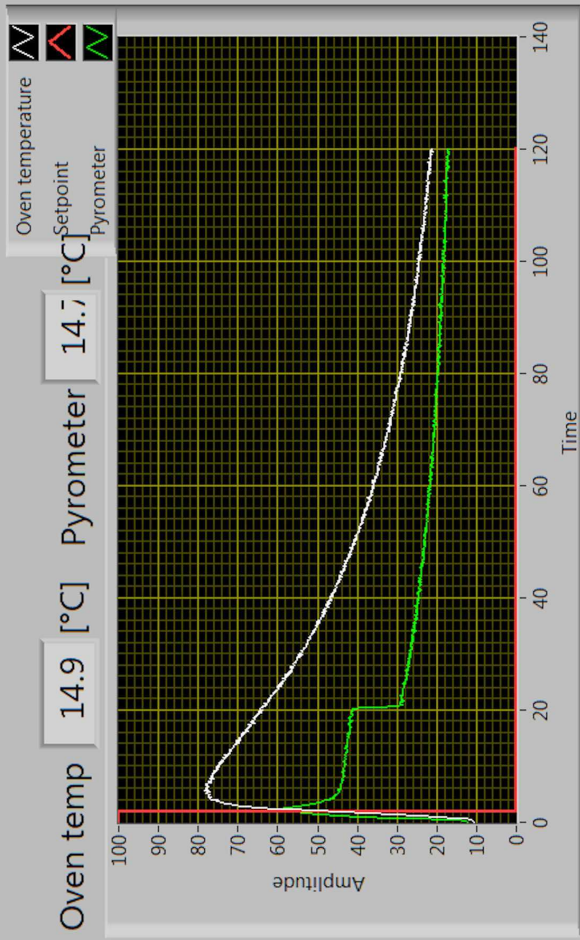


(a)



(b)





FIRA V2.2

Set point table

Pos	Time [ms]	FULL / OFF	Goto Po	Repeat N times
0	0	FULL		
1	2000	OFF		
2	120000	OFF		

START table STOP table Recall table Save table

table recalled: C:\Users\user\Documents\builds\

IR 1/2 3/4 5/6 OFF UV

SET Point manual 0 [°C] 0 [%]

Select Temperature Regulation FULL power / OFF Manual Table

timebase (min) 5000 Clear

Overheat Emergency STOP 23°C

Interloc IR case temperature 10 UV

PID O/P Limits 2 Valeur minimale 0.00 valeur maximale 10.00

Tracking window 10

PID PID Output 0.00

Parameters PID step

Proportional Kp 0.150 Integral Ki 0.0000 Derivative Kd 0.005

Proportional Kp 0.040 Integral Ki 0.0000 Derivative Kd 0.000

autotune? (F) Done

proportional gain (Kc) 0.150

integral time (Ti, min) 0.000

derivative time (Td, min) 0.005

Heat Capacity Cooling Rate Error Gain Delay (samples)

72.241 0.009 0.3 125

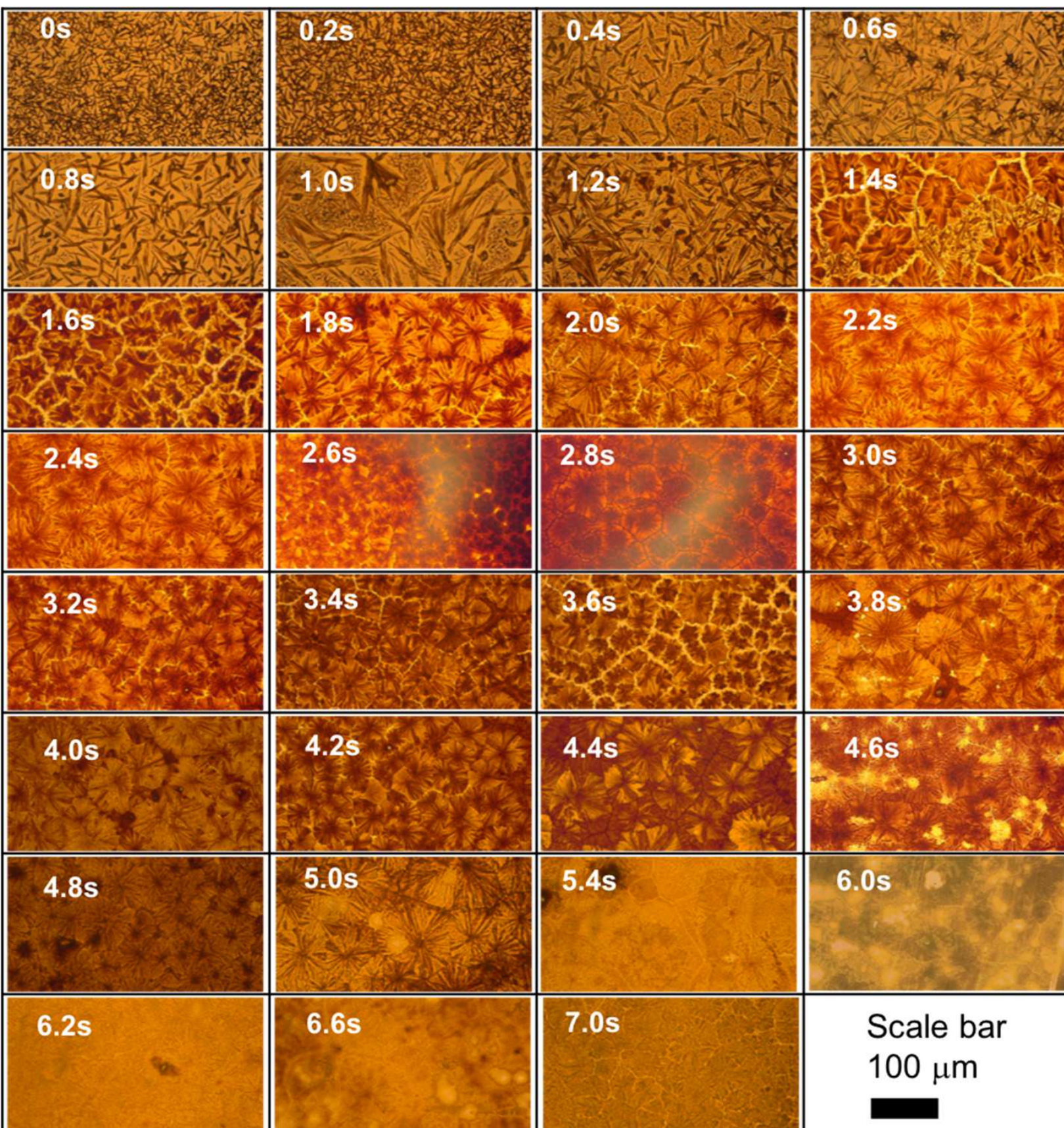
Control Valve Temperature

17520 0 176.30 2.9550

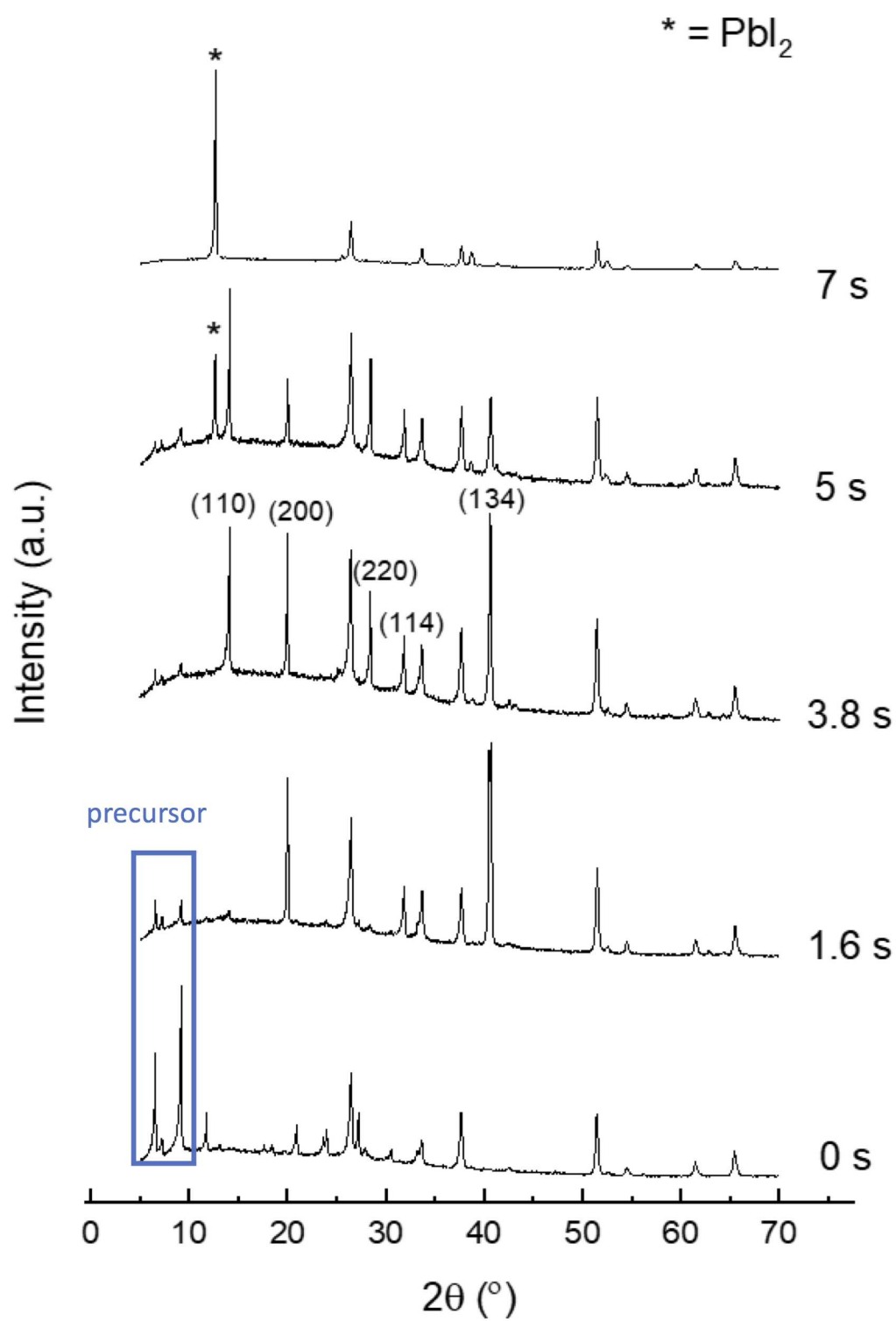
Dev1 ProductType USB-6001

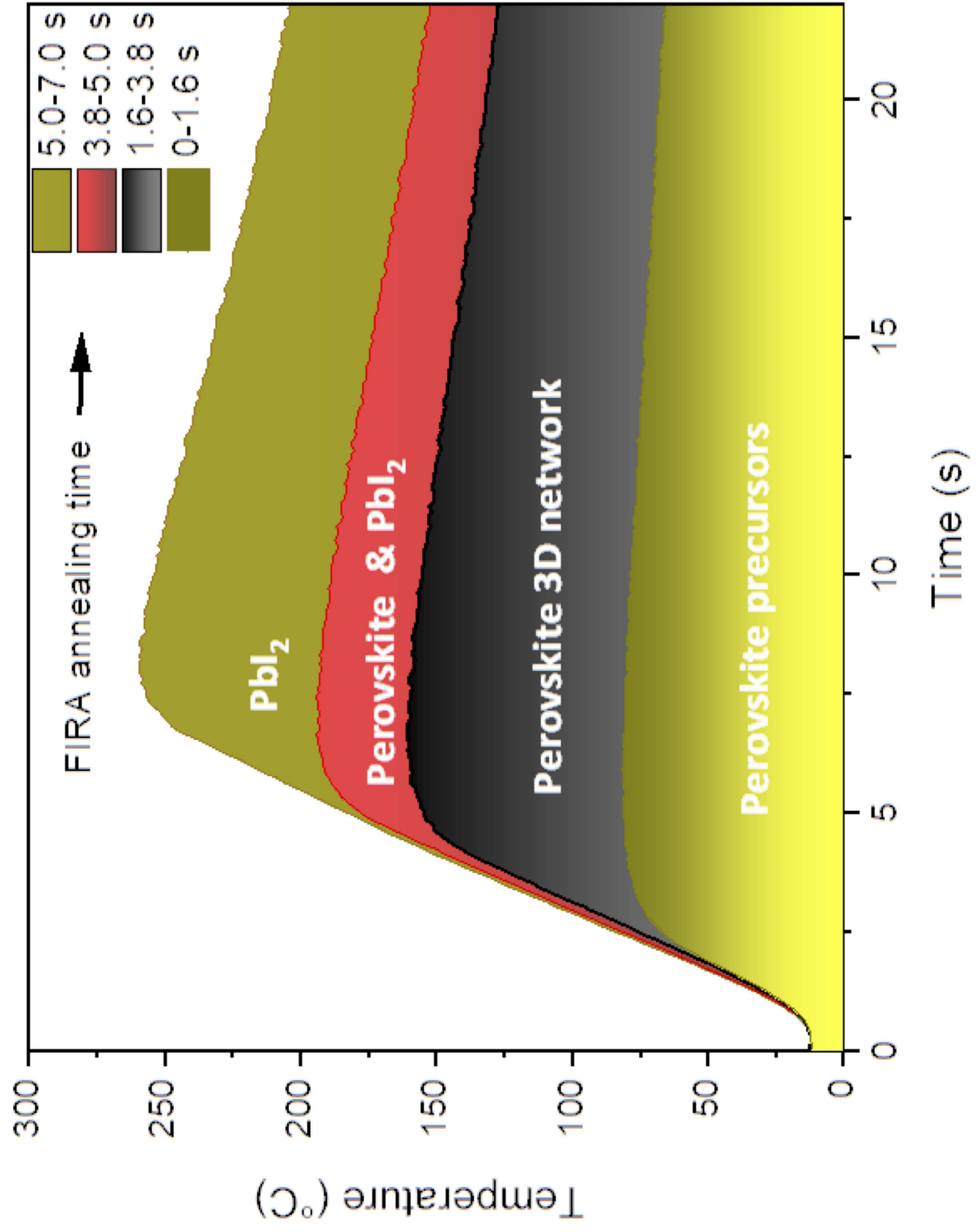
Dev1Simulated ProductType

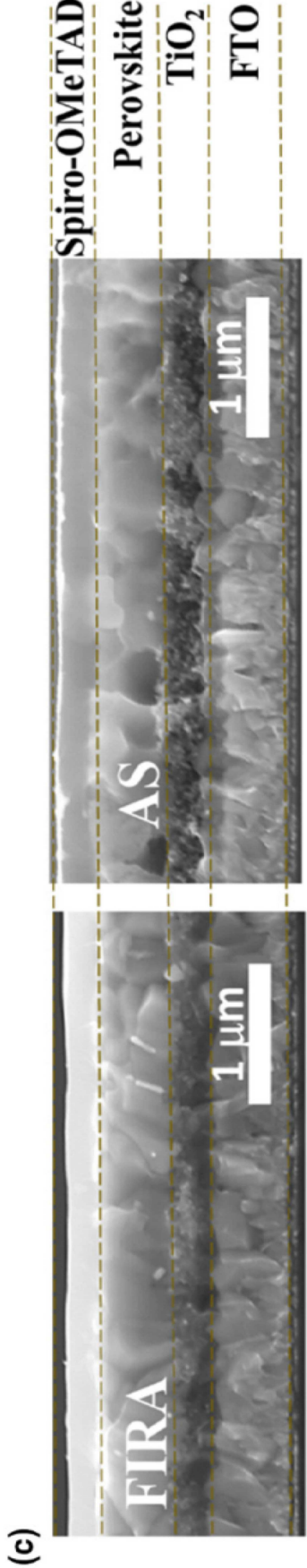
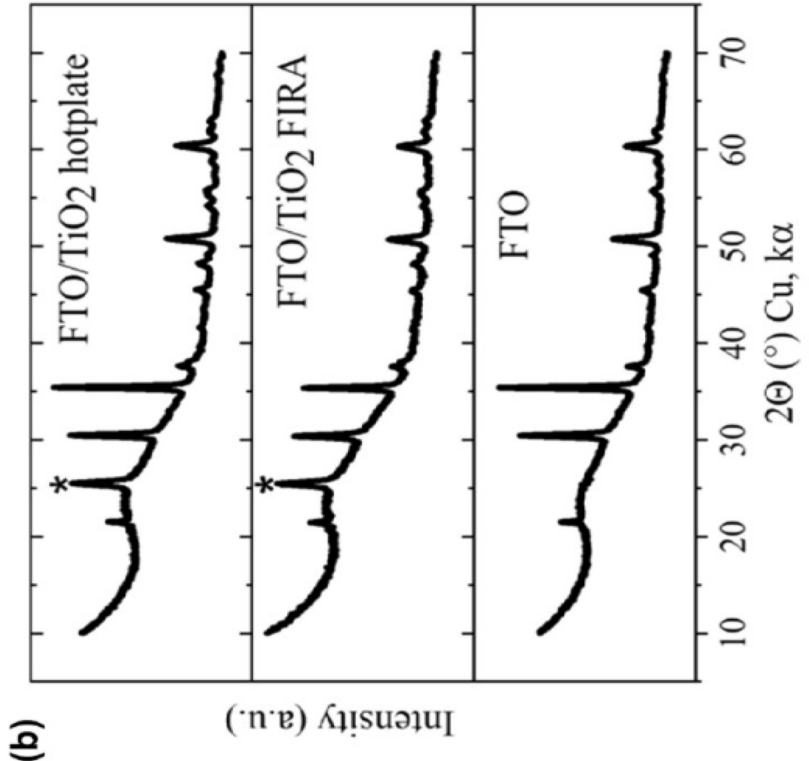
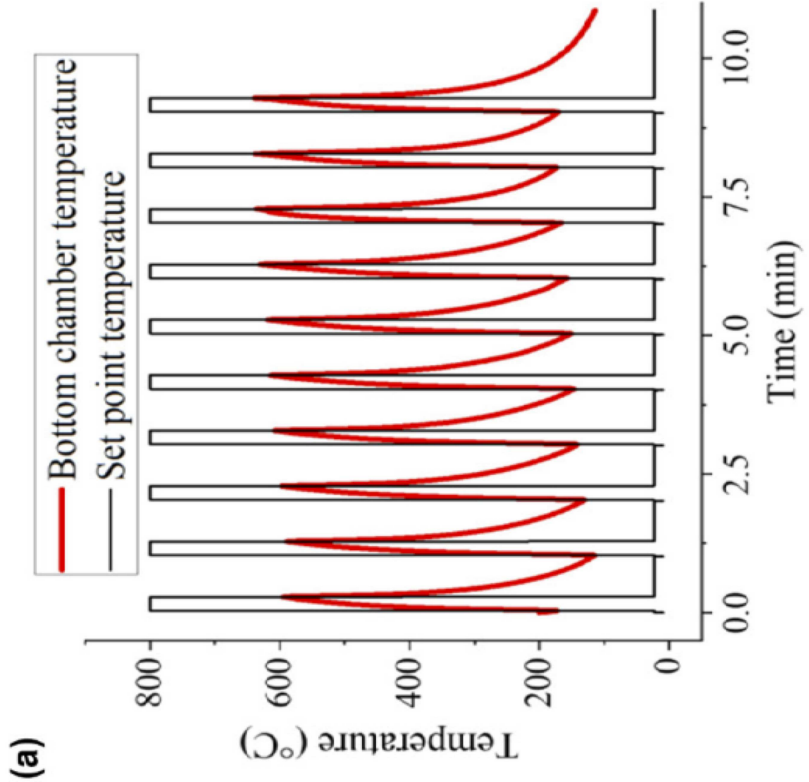


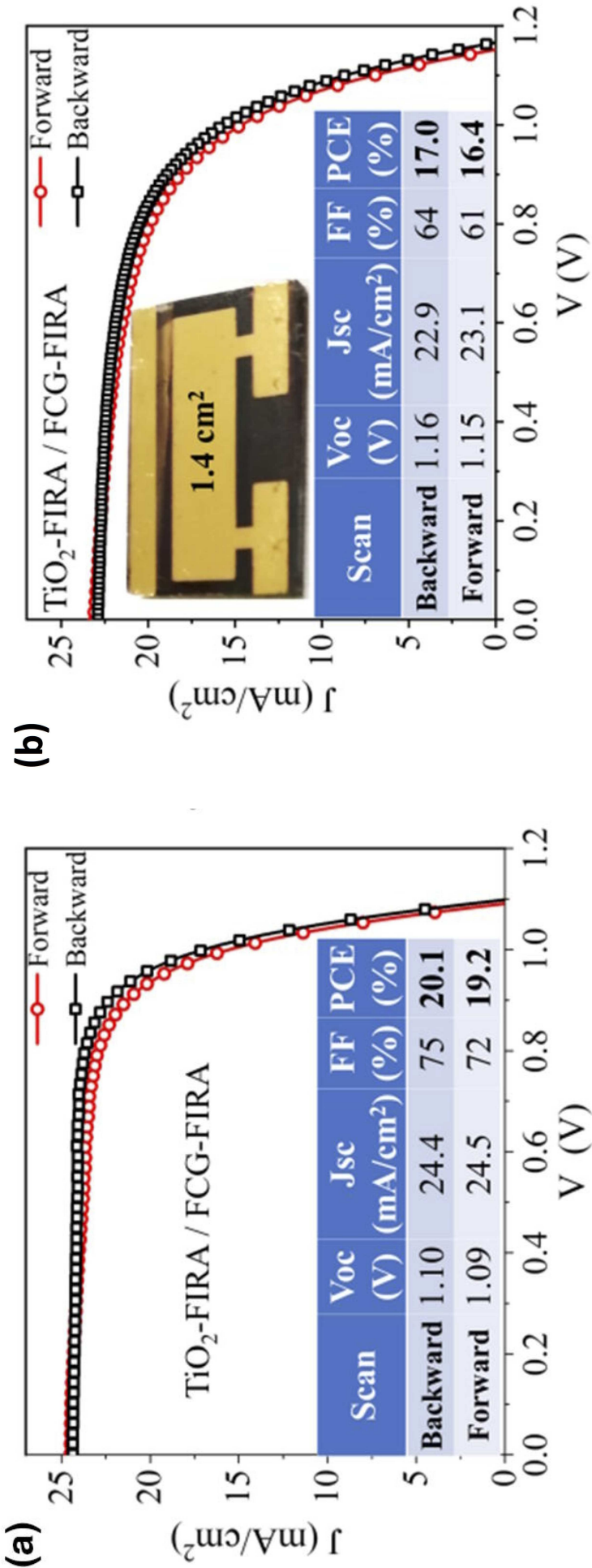




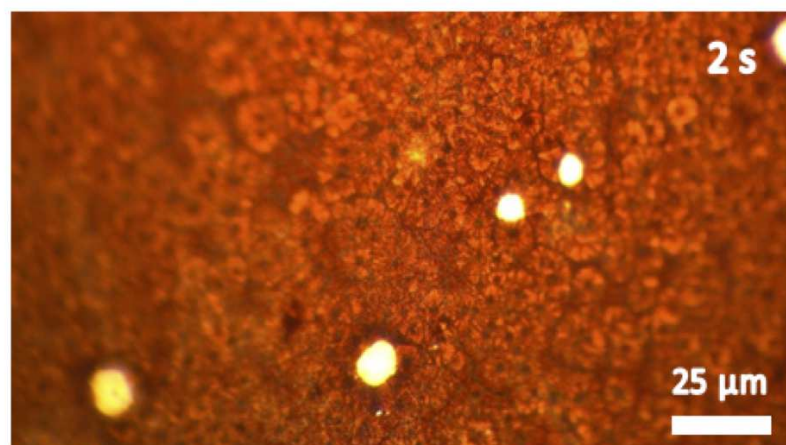
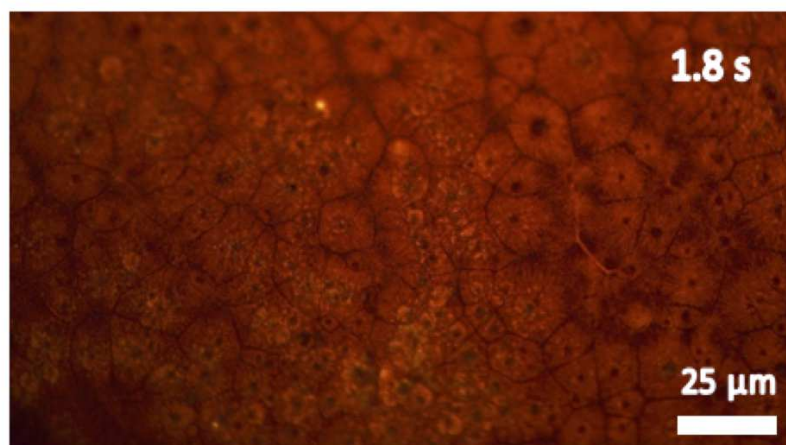
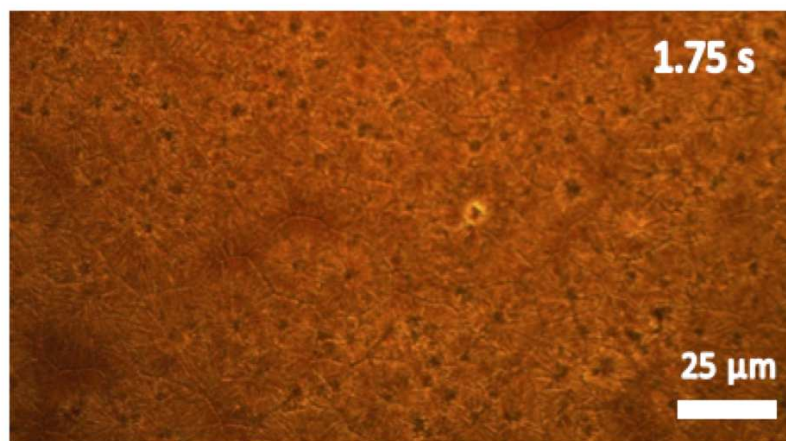
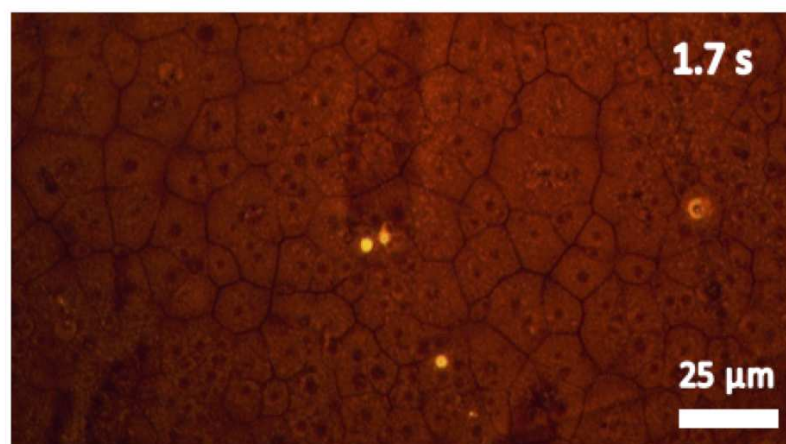
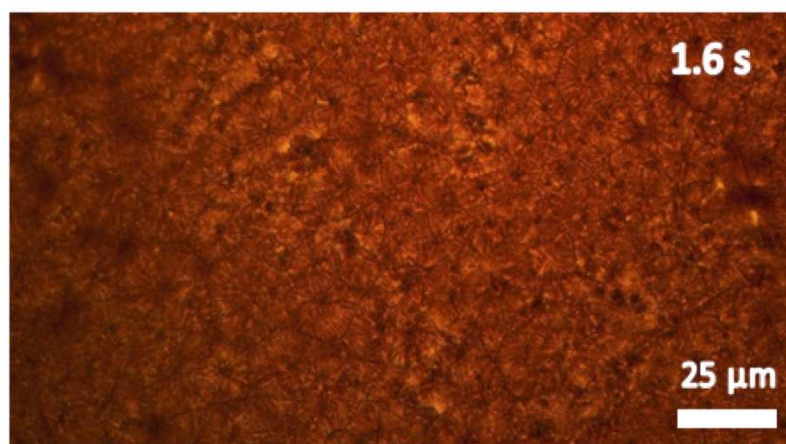
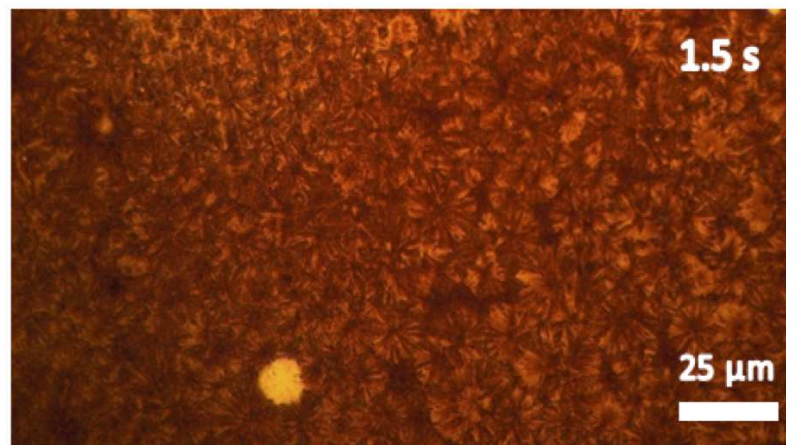




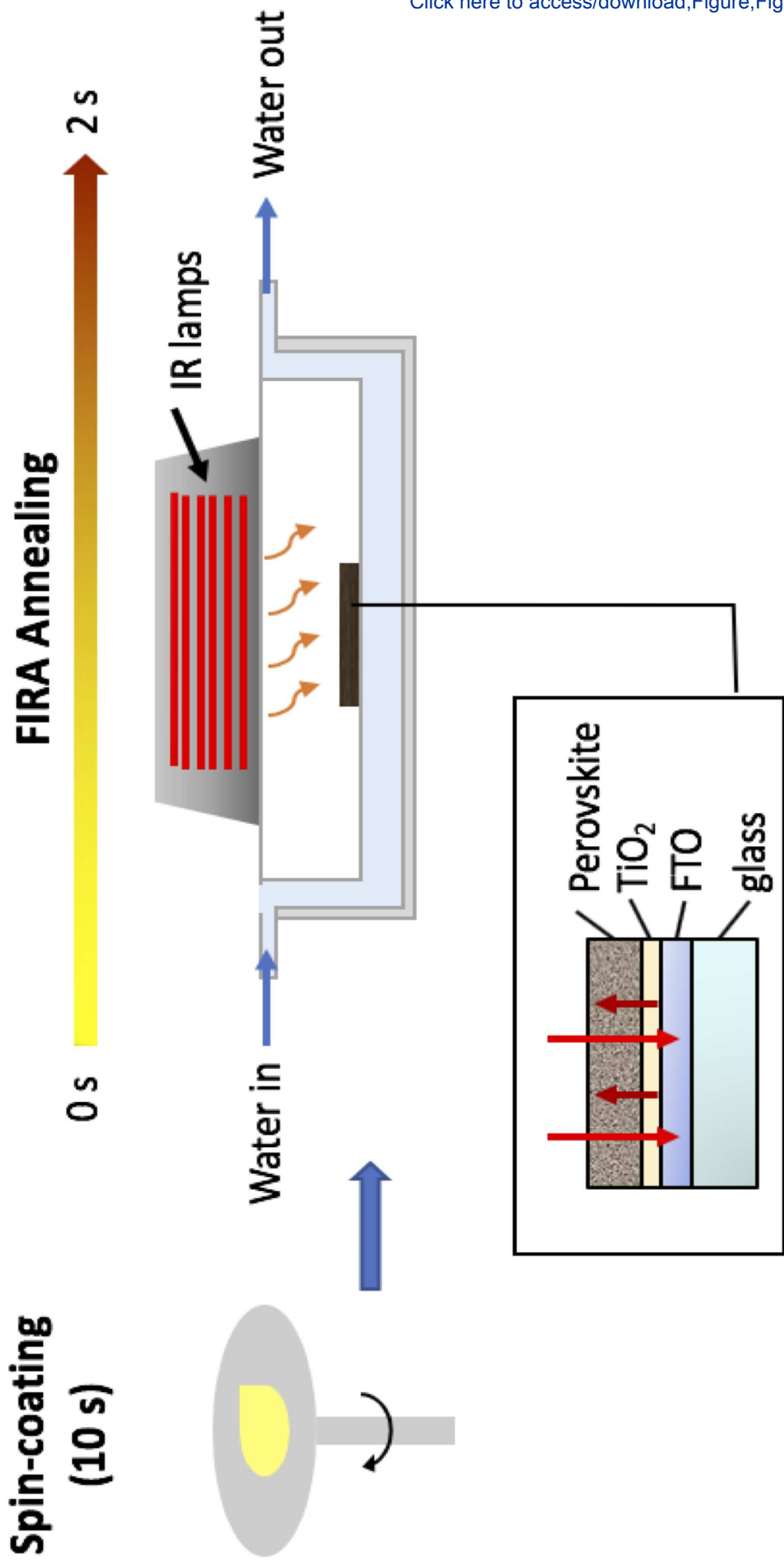


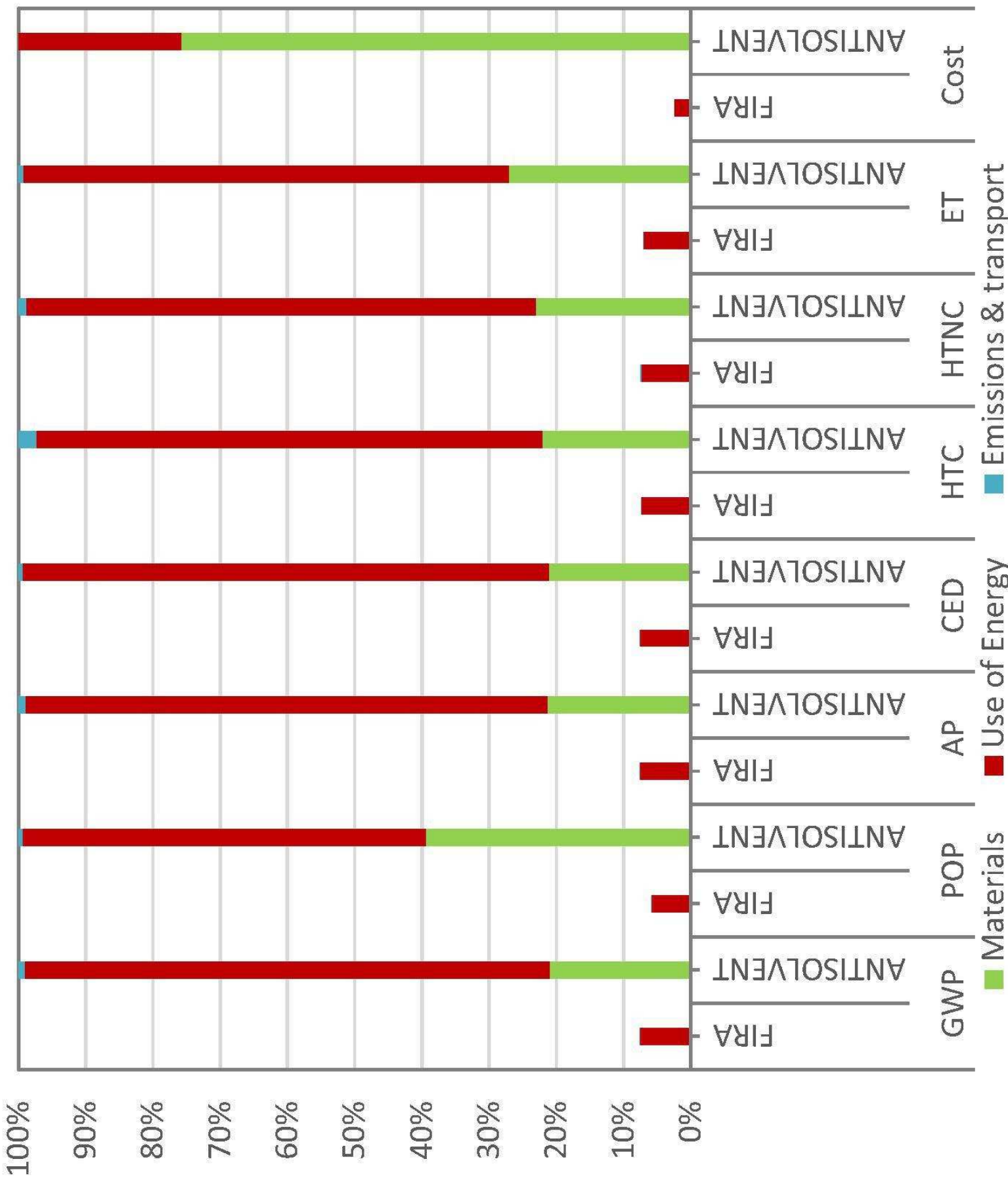












<b>Name of Material/ Equipment</b>	<b>Company</b>
4-tert-butylpyridine	Sigma Aldrich
Acetonitrile, anhydrous	ACROS Organics
Acetylacetone	Sigma Aldrich
Caesium iodide	Sigma Aldrich
Chlorobenzene, anhydrous	ACROS Organics
Digital source meter	Metrohm
DMF, anhydrous	ACROS Organics
DMSO, anhydrous	ACROS Organics
Ethanol	Sigma Aldrich
FIRA Software	Labview
FK209	Dyename
Formamidinium iodide	GreatCell Solar
FTO glass	Nippon Sheet Glass
Guanidinium iodide	Sigma Aldrich
Cleaning Soap	Hellmanex III
Hydrochloric acid	Sigma Aldrich
Isopropanol	Sigma Aldrich
ITO PET	Sigma Aldrich
Lead iodide	TCI
Li-TFSI	Sigma Aldrich
Mesoporous TiO <sub>2</sub> paste, 3 nrd	GreatCell Solar
Methylammonium iodide	GreatCell Solar
Microscope	Zeiss
Microscope lens	Zeiss
Microscope xenon light source	Ocean Optics
Optical fibre	Ocean Optics
Plasma cleaner	Jetlight Company Inc.
Polymer-planarised paper	Arjowiggins
Scanning electron microscope	Zeiss
Sintering hot plate	Harry Gestigkeit GMBH
Solar simulator	ABET Technologies

Spectrometer	Ocean Optics
Spiro-OMeTAD	Sigma Aldrich
Tetrabutyl ammonium iodide	GreatCell Solar
Thermal evaporator	Kurt J. Lesker
titanium diisopropoxide bis(acetylacetonate)	Sigma Aldrich
X-ray diffractometer	PANalytical
Zinc powder	Sigma Aldrich

Catalog Number	Comments/Description
142379	
AC610220010	
P7754	
203033	
AC396971000	
PGSTAT302N Autolab	
AC326871000	
AC326881000	
459844	
	Developed in-house
DN-P04	
SKU MS150000	
NSG 10	Sheet resistance = 11-13 ohms/sq
806056	
-	
320331	
190764	
639303	Sheet resistance = 60 ohms/sq
L0279	
544094	
SKU MS002300	
SKU MS1010000	
Axio-Scope A1 Polarizing Microscope	
EC Epiplan-Apochromat	
HPX-2000	
QP230-2-XSR	230 $\mu$ m core
UVO-Cleaner Model no. 256-220	
Powercoat HD	
Merlin Microscope	
-	
Model 11016 Sun 2000	

Maya2000 Pro  
792071  
SKU MS106000

Spectral range: 300-1100 nm

-  
325252  
mm)  
324930

equipped with a PIXcel-1D detector, Bragg-Brentano beam optics and parallel beam optic



5



## Response to Editorial and Reviewer Comments

RE: Submission “Flash Infrared Annealing Method for Perovskite Solar Cell Processing”

Dear Editor and Reviewers,

Thank you for taking the time to read our submission and for all your comments, they were very helpful and we have made changes to the manuscript accordingly. Attached please find a line-by-line response to your comments (in blue). We hope that we have adequately addressed all concerns raised.

Yours sincerely,  
Dr. Sandy Sanchez

### Editorial Comments

- Please take this opportunity to thoroughly proofread the manuscript to ensure that there are no spelling or grammatical errors.

We have thoroughly proofread the manuscript and corrected any errors that we found.

- **Protocol Language:** Please ensure that all text in the protocol section is written in the imperative voice/tense as if you are telling someone how to do the technique (i.e. “Do this”, “Measure that” etc.) Any text that cannot be written in the imperative tense may be added as a “Note”, however, notes should be used sparingly and actions should be described in the imperative tense wherever possible.

1) Some examples NOT in the imperative: 1.1.1, 1.1.4, 2.3.1 etc

This has been changed accordingly.

- **Protocol Detail:** Please note that your protocol will be used to generate the script for the video, and must contain everything that you would like shown in the video. **Please add more specific details (e.g. button clicks for software actions, numerical values for settings, etc) to your protocol steps.** There should be enough detail in each step to supplement the actions seen in the video so that viewers can easily replicate the protocol. Some examples:  
1) 1.2.1: Provide references for each.

We have included references for methods listed in 1.2.1 and added more specific details to the protocol steps.

- **Protocol Highlight:** Please highlight ~2.5 pages or less of text (which includes headings and spaces) in yellow, to identify which steps should be visualized to tell the most cohesive story of your protocol steps.

1) The highlighting must include all relevant details that are required to perform the step. For example, if step 2.5 is highlighted for filming and the details of how to perform the step are given in steps 2.5.1 and 2.5.2, then the sub-steps where the details are provided must be included in the highlighting.

- 2) The highlighted steps should form a cohesive narrative, that is, there must be a logical flow from one highlighted step to the next.
- 3) Please highlight complete sentences (not parts of sentences). Include sub-headings and spaces when calculating the final highlighted length.
- 4) Notes cannot be filmed and should be excluded from highlighting.

We have highlighted all the steps and corresponding sub-headings that we would like to film. Unfortunately, since we wanted to include a more general procedure in the protocol (sections 1-2) to give the readers an idea of the whole process before giving the protocol for more specific procedures, the highlighted parts are not strictly in logical order. For the video, we would like Section 2.3 Material Characterisation to be placed after Sections 3.3 and 3.4 in order to form a more cohesive narrative. Sorry for the inconvenience, but we believe this to be the best way to demonstrate the method and hope that this can be accommodated.

- **Results:** Remove the numbered list.

This has been removed.

- **Discussion:** JoVE articles are focused on the methods and the protocol, thus the discussion should be similarly focused. Please ensure that the discussion covers the following in detail and in paragraph form (3-6 paragraphs): 1) modifications and troubleshooting, 2) limitations of the technique, 3) significance with respect to existing methods, 4) future applications and 5) critical steps within the protocol.

We have added slightly more detail in the discussion and we believe that we have focused the discussion on the methods and the protocol:

- Paragraph 1: General discussion, critical steps in the protocol
- Paragraph 2: Modifications and future applications
- Paragraph 3: Limitations of the method, troubleshooting
- Paragraph 4: Significance with respect to existing methods
- Paragraph 5: Future applications

If there are any specific areas that require more explanation or elucidation, please let us know.

- **Figures:** Please remove the embedded figures from the manuscript. Figure legends, however, should remain within the manuscript text, directly below the Representative Results text.

This has been removed.

- **References:** Please spell out journal names.

This has been corrected

- **Commercial Language:** JoVE is unable to publish manuscripts containing commercial sounding language, including trademark or registered trademark symbols (TM/R) and the mention of company brand names before an instrument or reagent. Examples of

commercial sounding language in your manuscript are Hellmanex, LabView.

1) Please use MS Word's find function (Ctrl+F), to locate and replace all commercial sounding language in your manuscript with generic names that are not company-specific. All commercial products should be sufficiently referenced in the table of materials/reagents. You may use the generic term followed by "(see table of materials)" to draw the readers' attention to specific commercial names.

[This has been corrected](#)

- If your figures and tables are original and not published previously or you have already obtained figure permissions, please ignore this comment. If you are re-using figures from a previous publication, you must obtain explicit permission to re-use the figure from the previous publisher (this can be in the form of a letter from an editor or a link to the editorial policies that allows you to re-publish the figure). Please upload the text of the re-print permission (may be copied and pasted from an email/website) as a Word document to the Editorial Manager site in the "Supplemental files (as requested by JoVE)" section. Please also cite the figure appropriately in the figure legend, i.e. "This figure has been modified from [citation]."

[We have permission for all figures that have been previously published.](#)

#### Peer Review Comments

##### **Reviewer #1:**

##### **Manuscript Summary:**

This work reported a rapid thermal annealing process, so-called flash infrared annealing (FIRA), achieving high quality perovskite films for solar cells. This is an interesting work. Finally, a PCE = 20.1%, FF = 75%, VOC = 1.1 V and JSC = 24.4 mA/cm<sup>2</sup> were obtained. In addition, a PCE of large-area device with a 1.4 cm<sup>2</sup> was achieved to 17%.

##### **Major Concerns:**

There are few scientific discussions in this article. The authors only present what happened in each figure, rather than explain why.

##### **Minor Concerns:**

Some expressions are illogical, like "This paper firstly discusses the protocol used for the optimisation of annealing parameters to synthesise a compact, defect-free and homogeneous perovskite (MAPbI<sub>3</sub>) film". In fact, it's impossible to fabricate a perovskite film without any defect.

[Thank you for taking the time to read our submission and for your comments. Regarding your first point, we have decided to focus the discussion on the methodology, its advantages, disadvantages and potential, due to the nature of the journal being a process-focused one. We have included a simple explanation of the annealing process and the relationship between the annealing parameters and the resulting morphology in both the introduction \(paragraphs 3-5\) and the discussion \(paragraph 1\), and we have referenced many papers which give a more detailed scientific explanation of the underlying physical processes to supplement the](#)

readers' understanding. Regarding the second point, we have changed the wording in the manuscript.

#### **Reviewer #2:**

##### **Minor Concerns:**

The manuscript is well written and contains sufficient details for readers to follow the methods. I am happy for it being accepted for publication.

There is only one minor comment, the expression of "This method requires large amounts of organic solvent" on page 2 is a bit misleading and not accurate. The amount of anti-solvent used, for instance in spin-coating process is normally still in micro-litres (e.g., ~100uL for a 2x2cm substrate).

Thank you for taking the time to read our submission and for your comments. This is a good point, we have now changed the wording to "moderate amounts" and have indicated the ballpark amount used as suggested.

#### **Reviewer #3:**

The paper entitled Flash Infrared Annealing Method for Perovskite Solar Cell Processing submitted to the Journal of Visualized experiments demonstrate an important step in the transition of perovskite solar cells to a more scalable process and represents significant reduction in manufacturing time using radiative methods. The paper is well written and presented and illustrates the authors own methodology for achieving rapid heating using light based methods. As outlined in the conclusion it serves to illustrate the commercial opportunity for NIR processing, I particularly enjoyed figure 3 (optical images) and figure 5 (temperature profile) as examples of visually stimulating methods for demonstrating the potential.

The paper was an enjoyable read and should be published however it should be improved in a few ways in order to aid the reader, primarily to enhance the experimental richness of the process through more visual additions and through more prominent recognition of the history of light (and in particular NI radiation) in the fabrication of solar cells, where FIRA is used as a synonym for multipulse NIR radiation combined with substrate cooling.

The following recommendations should be considered by the authors prior to submission:

1. Given the complex nature of process and need for enhanced visualisation appropriate to the journal I would ask for the following to be included

- A visual image (still) of the apparatus beyond that which can be seen in the video clip
- Information on the nature of the equipment (e.g homemade or lab fabricated)
- Information on the nature of the illumination preferably an output spectrum. The authors postulate that the output is IR/UV however if these are tungsten halogen lamps then the output is likely to peak at around 1000 and therefore should be considered as near-infrared. This is key when considering possible free carrier excitation of the FTO.
- The power output density of the lamps per area

Thank you for taking the time to read our submission and for all your comments, we are very happy to have such a detailed review which has furthered our insight on the topic, and we would like to especially acknowledge your help in improving the quality of our submission. Regarding the above points:

- A visual image of the apparatus has now been included in Figure 1
- The equipment is homemade, we have now indicated this in the protocol (under section 1. Operation of the FIRA oven, p.3)
- We have added a few lines on the nature of the illumination (peak emission at 1073 nm) and the power output density of the lamps (3000 kW/m<sup>2</sup>) under section 1. Operation of the FIRA oven, p.3/4. We would like to clarify that the UV lamps mentioned in the discussion are a separate set of lamps that can be added to the apparatus and used instead of the NIR lamps.

2. The authors claim that it is a "low-temperature process". This is not the case, IR heating is used extensively for high temperature applications, in this experiment the temperature is high but the exposure duration is very low.

This is correct, it is instead a rapid thermal annealing process with rapid cooling. We have corrected this in the manuscript.

3. The authors claim that TiO<sub>2</sub> can be sintered using the FIRA process in many minutes, however there is extensive evidence demonstrating that TiO<sub>2</sub> can be sintered in a few seconds using this process, originally for dye-sensitized solar cells

(a) Watson, T.; Mabbett, I.; Wang, H.; Peter, L.; Worsley, D. Ultrafast near Infrared Sintering of TiO<sub>2</sub> Layers on Metal Substrates for Dye-Sensitized Solar Cells. *Prog. Photovoltaics Res. Appl.* 2011, 19 (4), 482-486.

(b) Hooper, K.; Carnie, M.; Charbonneau, C.; Watson, T. Near Infrared Radiation as a Rapid Heating Technique for TiO<sub>2</sub> Films on Glass Mounted Dye-Sensitized Solar Cells. *Int. J. Photoenergy* 2014, 2014, 953623.

(c) Carnie, M. J.; Charbonneau, C.; Barnes, P. R. F.; Davies, M. L.; Mabbett, I.; Watson, T. M.; O'Regan, B. C.; Worsley, D. A. Ultra-Fast Sintered TiO<sub>2</sub> Films in Dye-Sensitized Solar Cells: Phase Variation, Electron Transport and Recombination. *J. Mater. Chem. A* 2013, 1 (6), 2225.

And more recently for perovskite solar cells

(d) Baker, J.; Hooper, K.; Meroni, S.; Pockett, A.; McGettrick, J.; Wei, Z.; Escalante, R.; Oskam, G.; Carnie, M.; Watson, T. High Throughput Fabrication of Mesoporous Carbon Perovskite Solar Cells. *J. Mater. Chem. A* 2017, 5 (35), 18643-18650.

Indeed, we have now included the above point and references in the manuscript.

4. Where FIRA is used on flexible substrates it should be noted that the absorption of the film will change as the material transitions from non-absorbing (wet NIR transparent perovskite precursor material) to dry (NIR absorbing black) and it this additional absorption

when black that is likely to be reason for the damage to the substrate, beyond the chamber itself becoming hot. This is detailed in a similar way for the NIR processing of PEDOT:PSS

(e) Bryant, D.; Mabbett, I.; Greenwood, P.; Watson, T.; Wijdekop, M.; Worsley, D. Ultrafast Near-Infrared Curing of PEDOT:PSS. *Org. Electron. physics, Mater. Appl.* 2014, 15 (6).

Thank you for pointing this out. We agree that there is an additional contribution from the solid-black perovskite absorption, and we have added this comment to the manuscript as well as the suggested references for clarification.

5. What is the location of the thermocouple? If the thermocouple is directly exposed to the light output then this will independently heat-up skewing the overall chamber results. How confident are the authors that the temperature logging system?

This is a key point. In fact, we have two k-type thermocouples, one exposed to IR radiation (in the centre of the chamber) and the second below the bottom of the annealing chamber. In addition, we have an infrared sensor that directly measures the surface of the sample, with a germanium window to block the excess of IR radiation. Then, with the three sensors we can establish a temperature gradient for the heat transfer, knowing the temperature in different positions of the chamber (on the Z axis with respect to the horizontal bottom). However, for our database systematically, we use temperature values measured by the thermocouple directly exposed to IR as a reference for all our processes, which does not match with the temperature measured in the standard hotplate annealing process e.g the perovskite phase transition temperature. We have added a clarification for this in a NOTE under Section 1.1 (p.4).

## ELSEVIER LICENSE TERMS AND CONDITIONS

Sep 27, 2020

---

---

This Agreement between EPFL -- Sandy Sánchez ("You") and Elsevier ("Elsevier") consists of your license details and the terms and conditions provided by Elsevier and Copyright Clearance Center.

License Number 4917010429162

License date Sep 27, 2020

Licensed Content  
Publisher Elsevier

Licensed Content  
Publication Materials Today

Licensed Content Title Flash infrared annealing as a cost-effective and low  
environmental impact processing method for planar perovskite  
solar cells

Licensed Content Author Sandy Sánchez,Marta Vallés-Pelarda,Jaume-Adrià Alberola-  
Borràs,Rosario Vidal,José J. Jerónimo-Rendón,Michael  
Saliba,Pablo P. Boix,Iván Mora-Seró

Licensed Content Date Dec 1, 2019

Licensed Content Volume 31

Licensed Content Issue n/a

Licensed Content Pages 8

Start Page 39

End Page 46

Type of Use	reuse in a journal/magazine
Requestor type	academic/educational institute
Portion	figures/tables/illustrations
Number of figures/tables/illustrations	1
Format	electronic
Are you the author of this Elsevier article?	Yes
Will you be translating?	No
Title of new article	Flash Infrared Annealing for Perovskite Solar Cell Processing
Lead author	sandy sanchez alonso
Title of targeted journal	JOVE
Publisher	MyJOVE
Expected publication date	Nov 2020
Portions	Figure 6
Requestor Location	EPFL EPFL SB ISIC LSPM CH B2 424 (Bâtiment CH) Station 6 Lausanne, Vaud 1015 Switzerland Attn: EPFL
Publisher Tax ID	GB 494 6272 12
Total	0.00 USD
Terms and Conditions	



## INTRODUCTION

1. The publisher for this copyrighted material is Elsevier. By clicking "accept" in connection with completing this licensing transaction, you agree that the following terms and conditions apply to this transaction (along with the Billing and Payment terms and conditions established by Copyright Clearance Center, Inc. ("CCC"), at the time that you opened your Rightslink account and that are available at any time at <http://myaccount.copyright.com>).

## GENERAL TERMS

2. Elsevier hereby grants you permission to reproduce the aforementioned material subject to the terms and conditions indicated.

3. Acknowledgement: If any part of the material to be used (for example, figures) has appeared in our publication with credit or acknowledgement to another source, permission must also be sought from that source. If such permission is not obtained then that material may not be included in your publication/copies. Suitable acknowledgement to the source must be made, either as a footnote or in a reference list at the end of your publication, as follows:

"Reprinted from Publication title, Vol /edition number, Author(s), Title of article / title of chapter, Pages No., Copyright (Year), with permission from Elsevier [OR APPLICABLE SOCIETY COPYRIGHT OWNER]." Also Lancet special credit - "Reprinted from The Lancet, Vol. number, Author(s), Title of article, Pages No., Copyright (Year), with permission from Elsevier."

4. Reproduction of this material is confined to the purpose and/or media for which permission is hereby given.

5. Altering/Modifying Material: Not Permitted. However figures and illustrations may be altered/adapted minimally to serve your work. Any other abbreviations, additions, deletions and/or any other alterations shall be made only with prior written authorization of Elsevier Ltd. (Please contact Elsevier's permissions helpdesk [here](#)). No modifications can be made to any Lancet figures/tables and they must be reproduced in full.

6. If the permission fee for the requested use of our material is waived in this instance, please be advised that your future requests for Elsevier materials may attract a fee.

7. Reservation of Rights: Publisher reserves all rights not specifically granted in the combination of (i) the license details provided by you and accepted in the course of this licensing transaction, (ii) these terms and conditions and (iii) CCC's Billing and Payment terms and conditions.

8. License Contingent Upon Payment: While you may exercise the rights licensed immediately upon issuance of the license at the end of the licensing process for the transaction, provided that you have disclosed complete and accurate details of your proposed use, no license is finally effective unless and until full payment is received from you (either by publisher or by CCC) as provided in CCC's Billing and Payment terms and conditions. If full payment is not received on a timely basis, then any license preliminarily granted shall be deemed automatically revoked and shall be void as if never granted. Further, in the event that you breach any of these terms and conditions or any of CCC's Billing and Payment terms and conditions, the license is automatically revoked and shall be void as if never granted. Use of materials as described in a revoked license, as well as any use of the materials beyond the scope of an unrevoked license, may constitute copyright infringement and publisher reserves the right to take any and all action to protect its copyright in the materials.

9. Warranties: Publisher makes no representations or warranties with respect to the licensed material.

10. Indemnity: You hereby indemnify and agree to hold harmless publisher and CCC, and their respective officers, directors, employees and agents, from and against any and all claims arising out of your use of the licensed material other than as specifically authorized pursuant to this license.

11. No Transfer of License: This license is personal to you and may not be sublicensed, assigned, or transferred by you to any other person without publisher's written permission.

12. No Amendment Except in Writing: This license may not be amended except in a writing signed by both parties (or, in the case of publisher, by CCC on publisher's behalf).

13. Objection to Contrary Terms: Publisher hereby objects to any terms contained in any purchase order, acknowledgment, check endorsement or other writing prepared by you, which terms are inconsistent with these terms and conditions or CCC's Billing and Payment terms and conditions. These terms and conditions, together with CCC's Billing and Payment terms and conditions (which are incorporated herein), comprise the entire agreement between you and publisher (and CCC) concerning this licensing transaction. In the event of any conflict between your obligations established by these terms and conditions and those established by CCC's Billing and Payment terms and conditions, these terms and conditions shall control.

14. Revocation: Elsevier or Copyright Clearance Center may deny the permissions described in this License at their sole discretion, for any reason or no reason, with a full refund payable to you. Notice of such denial will be made using the contact information provided by you. Failure to receive such notice will not alter or invalidate the denial. In no event will Elsevier or Copyright Clearance Center be responsible or liable for any costs, expenses or damage incurred by you as a result of a denial of your permission request, other than a refund of the amount(s) paid by you to Elsevier and/or Copyright Clearance Center for denied permissions.

### LIMITED LICENSE

The following terms and conditions apply only to specific license types:

15. **Translation:** This permission is granted for non-exclusive world **English** rights only unless your license was granted for translation rights. If you licensed translation rights you may only translate this content into the languages you requested. A professional translator must perform all translations and reproduce the content word for word preserving the integrity of the article.

16. **Posting licensed content on any Website:** The following terms and conditions apply as follows: Licensing material from an Elsevier journal: All content posted to the web site must maintain the copyright information line on the bottom of each image; A hyper-text must be included to the Homepage of the journal from which you are licensing at <http://www.sciencedirect.com/science/journal/xxxxx> or the Elsevier homepage for books at <http://www.elsevier.com>; Central Storage: This license does not include permission for a scanned version of the material to be stored in a central repository such as that provided by Heron/XanEdu.

Licensing material from an Elsevier book: A hyper-text link must be included to the Elsevier homepage at <http://www.elsevier.com>. All content posted to the web site must maintain the copyright information line on the bottom of each image.

**Posting licensed content on Electronic reserve:** In addition to the above the following clauses are applicable: The web site must be password-protected and made available only to bona fide students registered on a relevant course. This permission is granted for 1 year only. You may obtain a new license for future website posting.

**17. For journal authors:** the following clauses are applicable in addition to the above:

### **Preprints:**

A preprint is an author's own write-up of research results and analysis, it has not been peer-reviewed, nor has it had any other value added to it by a publisher (such as formatting, copyright, technical enhancement etc.).

Authors can share their preprints anywhere at any time. Preprints should not be added to or enhanced in any way in order to appear more like, or to substitute for, the final versions of articles however authors can update their preprints on arXiv or RePEc with their Accepted Author Manuscript (see below).

If accepted for publication, we encourage authors to link from the preprint to their formal publication via its DOI. Millions of researchers have access to the formal publications on ScienceDirect, and so links will help users to find, access, cite and use the best available version. Please note that Cell Press, The Lancet and some society-owned have different preprint policies. Information on these policies is available on the journal homepage.

**Accepted Author Manuscripts:** An accepted author manuscript is the manuscript of an article that has been accepted for publication and which typically includes author-incorporated changes suggested during submission, peer review and editor-author communications.

Authors can share their accepted author manuscript:

- immediately
  - via their non-commercial person homepage or blog
  - by updating a preprint in arXiv or RePEc with the accepted manuscript
  - via their research institute or institutional repository for internal institutional uses or as part of an invitation-only research collaboration work-group
  - directly by providing copies to their students or to research collaborators for their personal use
  - for private scholarly sharing as part of an invitation-only work group on commercial sites with which Elsevier has an agreement
- After the embargo period
  - via non-commercial hosting platforms such as their institutional repository
  - via commercial sites with which Elsevier has an agreement

In all cases accepted manuscripts should:

- link to the formal publication via its DOI
- bear a CC-BY-NC-ND license - this is easy to do
- if aggregated with other manuscripts, for example in a repository or other site, be shared in alignment with our hosting policy not be added to or enhanced in any way to appear more like, or to substitute for, the published journal article.

**Published journal article (JPA):** A published journal article (PJA) is the definitive final record of published research that appears or will appear in the journal and embodies all value-adding publishing activities including peer review co-ordination, copy-editing, formatting, (if relevant) pagination and online enrichment.

Policies for sharing publishing journal articles differ for subscription and gold open access articles:

**Subscription Articles:** If you are an author, please share a link to your article rather than the full-text. Millions of researchers have access to the formal publications on ScienceDirect, and so links will help your users to find, access, cite, and use the best available version.

Theses and dissertations which contain embedded PJAs as part of the formal submission can be posted publicly by the awarding institution with DOI links back to the formal publications on ScienceDirect.

If you are affiliated with a library that subscribes to ScienceDirect you have additional private sharing rights for others' research accessed under that agreement. This includes use for classroom teaching and internal training at the institution (including use in course packs and courseware programs), and inclusion of the article for grant funding purposes.

**Gold Open Access Articles:** May be shared according to the author-selected end-user license and should contain a [CrossMark logo](#), the end user license, and a DOI link to the formal publication on ScienceDirect.

Please refer to Elsevier's [posting policy](#) for further information.

**18. For book authors** the following clauses are applicable in addition to the above: Authors are permitted to place a brief summary of their work online only. You are not allowed to download and post the published electronic version of your chapter, nor may you scan the printed edition to create an electronic version. **Posting to a repository:** Authors are permitted to post a summary of their chapter only in their institution's repository.

**19. Thesis/Dissertation:** If your license is for use in a thesis/dissertation your thesis may be submitted to your institution in either print or electronic form. Should your thesis be published commercially, please reapply for permission. These requirements include permission for the Library and Archives of Canada to supply single copies, on demand, of the complete thesis and include permission for Proquest/UMI to supply single copies, on demand, of the complete thesis. Should your thesis be published commercially, please reapply for permission. Theses and dissertations which contain embedded PJAs as part of the formal submission can be posted publicly by the awarding institution with DOI links back to the formal publications on ScienceDirect.

### **Elsevier Open Access Terms and Conditions**

You can publish open access with Elsevier in hundreds of open access journals or in nearly 2000 established subscription journals that support open access publishing. Permitted third party re-use of these open access articles is defined by the author's choice of Creative Commons user license. See our [open access license policy](#) for more information.

### **Terms & Conditions applicable to all Open Access articles published with Elsevier:**

Any reuse of the article must not represent the author as endorsing the adaptation of the article nor should the article be modified in such a way as to damage the author's honour or reputation. If any changes have been made, such changes must be clearly indicated.

The author(s) must be appropriately credited and we ask that you include the end user license and a DOI link to the formal publication on ScienceDirect.

If any part of the material to be used (for example, figures) has appeared in our publication with credit or acknowledgement to another source it is the responsibility of the user to ensure their reuse complies with the terms and conditions determined by the rights holder.

### **Additional Terms & Conditions applicable to each Creative Commons user license:**

**CC BY:** The CC-BY license allows users to copy, to create extracts, abstracts and new works from the Article, to alter and revise the Article and to make commercial use of the Article (including reuse and/or resale of the Article by commercial entities), provided the user gives appropriate credit (with a link to the formal publication through the relevant

DOI), provides a link to the license, indicates if changes were made and the licensor is not represented as endorsing the use made of the work. The full details of the license are available at <http://creativecommons.org/licenses/by/4.0>.

**CC BY NC SA:** The CC BY-NC-SA license allows users to copy, to create extracts, abstracts and new works from the Article, to alter and revise the Article, provided this is not done for commercial purposes, and that the user gives appropriate credit (with a link to the formal publication through the relevant DOI), provides a link to the license, indicates if changes were made and the licensor is not represented as endorsing the use made of the work. Further, any new works must be made available on the same conditions. The full details of the license are available at <http://creativecommons.org/licenses/by-nc-sa/4.0>.

**CC BY NC ND:** The CC BY-NC-ND license allows users to copy and distribute the Article, provided this is not done for commercial purposes and further does not permit distribution of the Article if it is changed or edited in any way, and provided the user gives appropriate credit (with a link to the formal publication through the relevant DOI), provides a link to the license, and that the licensor is not represented as endorsing the use made of the work. The full details of the license are available at <http://creativecommons.org/licenses/by-nc-nd/4.0>. Any commercial reuse of Open Access articles published with a CC BY NC SA or CC BY NC ND license requires permission from Elsevier and will be subject to a fee.

Commercial reuse includes:

- Associating advertising with the full text of the Article
- Charging fees for document delivery or access
- Article aggregation
- Systematic distribution via e-mail lists or share buttons

Posting or linking by commercial companies for use by customers of those companies.

## 20. Other Conditions:

v1.10

Questions? [customercare@copyright.com](mailto:customercare@copyright.com) or +1-855-239-3415 (toll free in the US) or +1-978-646-2777.

# Flash Infrared Annealing Method for Perovskite Solar Cell Processing

## Supporting Information

*Pui Sha Victoria Ling<sup>1,2</sup>, Anders Hagfeldt<sup>2\*</sup>, Sandy Sanchez,<sup>2\*</sup>*

1: Department of Chemistry, Molecular Sciences Research Hub, Imperial College London,  
80 Wood Lane, Shepherd's Bush, London, W12 0BZ, United Kingdom

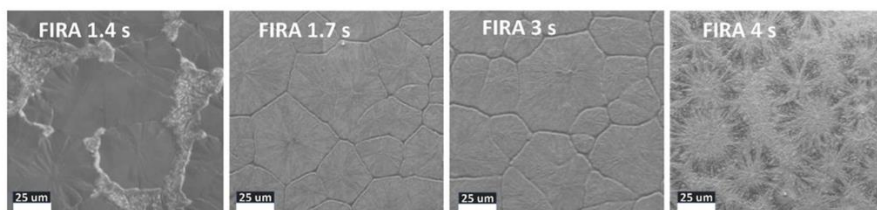
2: Laboratory of Photomolecular Science (LSPM), École Polytechnique Fédérale de  
Lausanne (EPFL), 1015 Lausanne, Switzerland

\*Corresponding author:

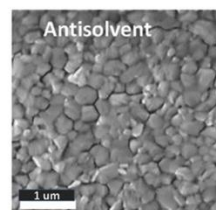
[sandy.sanchezalonso@epfl.ch](mailto:sandy.sanchezalonso@epfl.ch), [anders.hagfeldt@epfl.ch](mailto:anders.hagfeldt@epfl.ch)

S1. a) Top view of FIRA- annealed perovskite films for four annealing times, scale bar: 25  $\mu\text{m}$ . b) Top view of a reference film made by the antisolvent method followed by annealing at 100  $^{\circ}\text{C}$  for 1 h on a standard hotplate. Adapted from<sup>1</sup>.

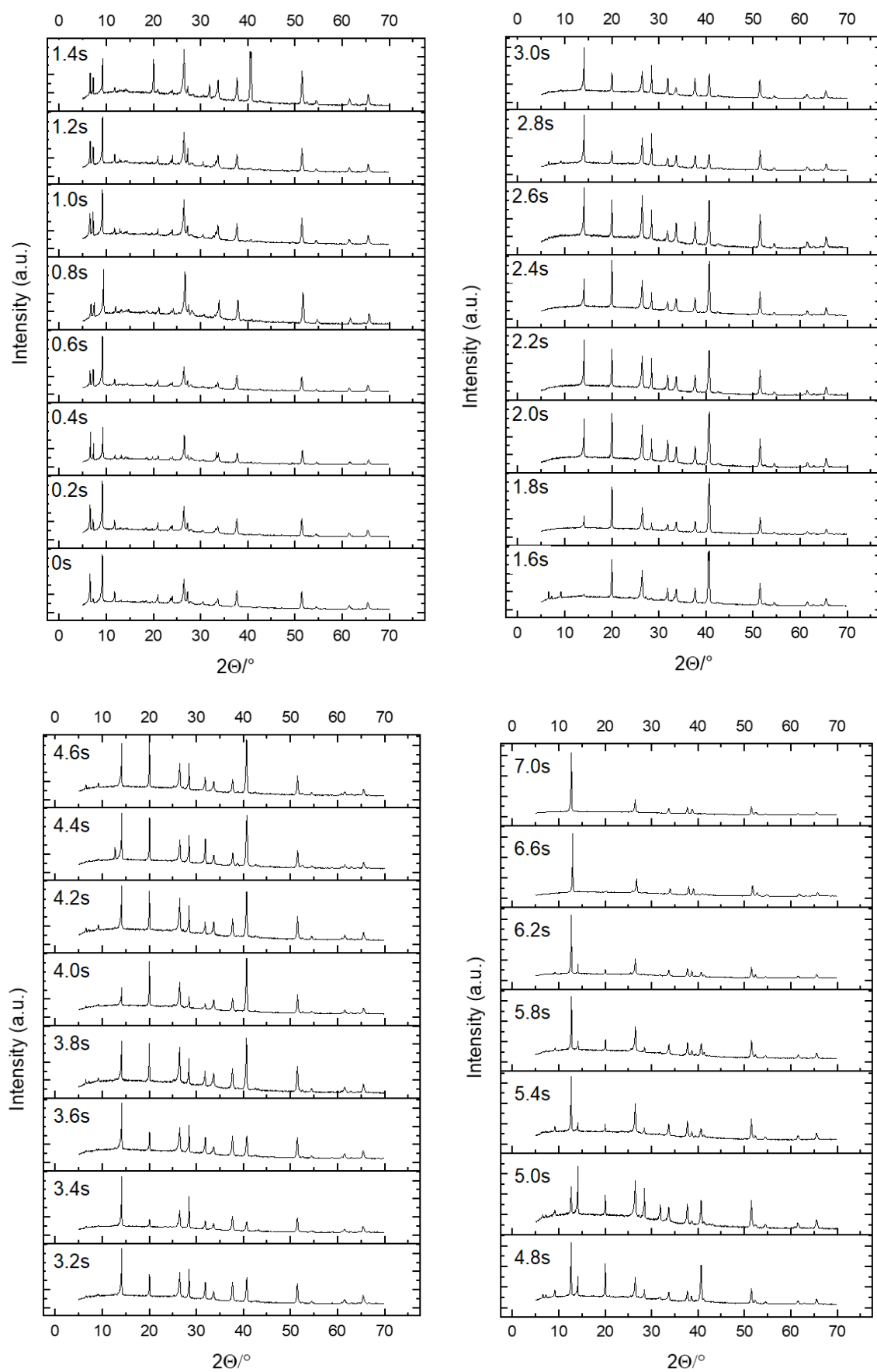
**a**



**b**

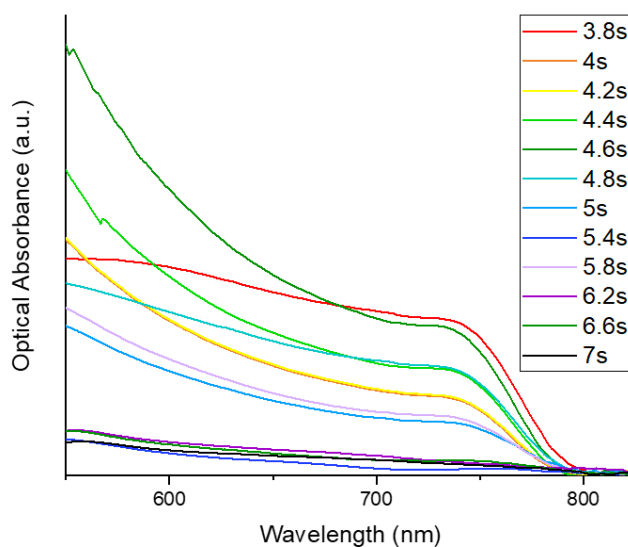
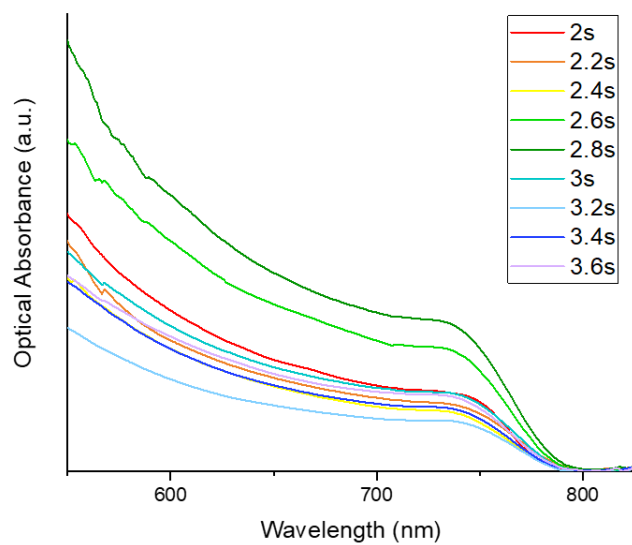
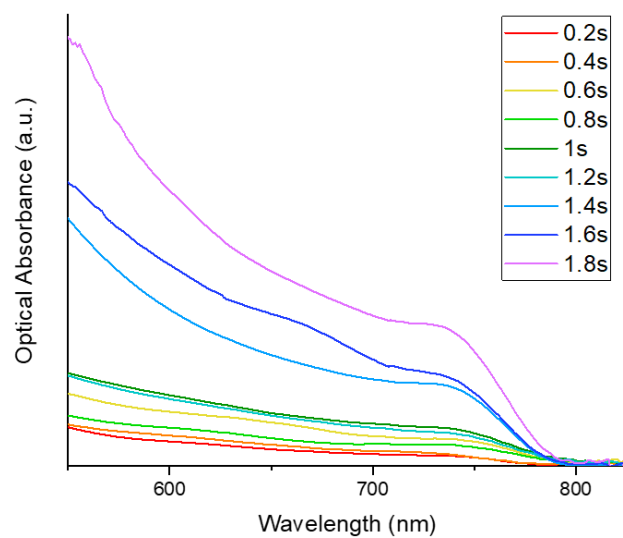


## S2. XRD spectra of MAPbI<sub>3</sub> films on FTO glass, annealed with pulses of 0 s to 7 s

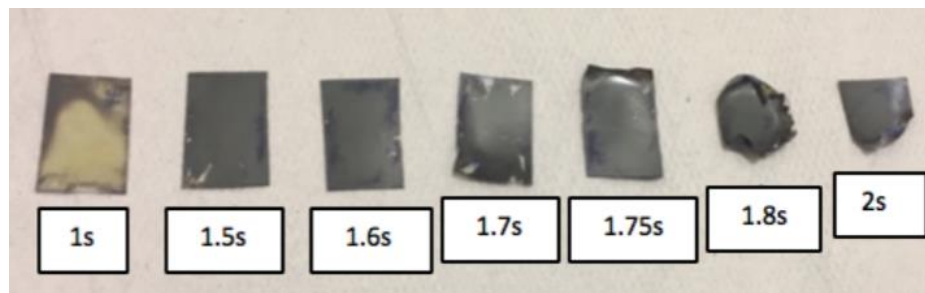




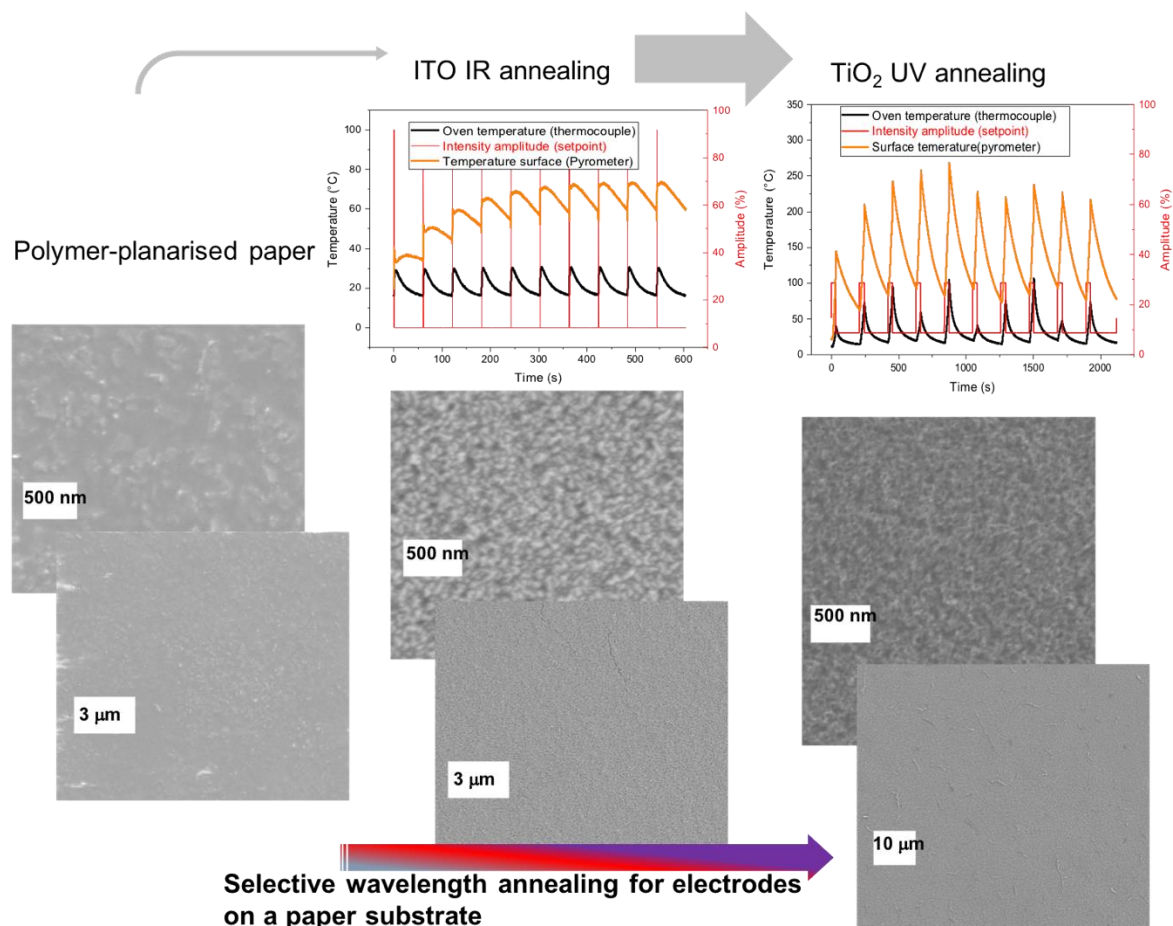
S3. Absorbance spectra of MAPbI<sub>3</sub> films on FTO glass, annealed with pulses of 0 s to 7 s



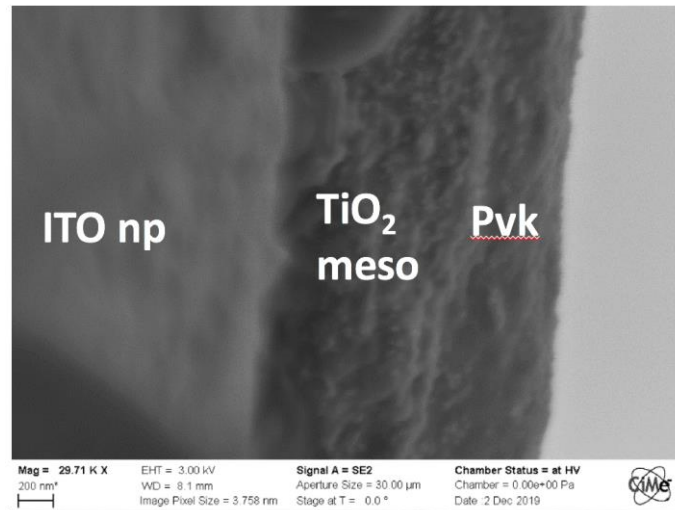
S4. Physical appearance of MAPbI<sub>3</sub> films annealed on PET at various pulse lengths



S5. Temperature profile and top-view SEM images of the pristine paper substrate, ITO electrode and mesoporous-TiO<sub>2</sub> layer processed with FIRA



S6. Cross-sectional SEM image of perovskite deposited (via antisolvent method) on a FIRA-annealed ITO/TiO<sub>2</sub> stack.



\*ITO np = ITO nanoparticles, pvk = perovskite